THE APPLICABILITY OF REMOTE SENSING METHODS FOR THE DETECTION OF FIRES ON COAL DISCARD DUMPS

Pratibha Mistry

A project report submitted to the Faculty of Engineering and the Built Environment, University of the Witwatersrand, in partial fulfilment of the requirements for the degree of Master of Science in Engineering.

Johannesburg, 2005

Declaration

I declare that this research report is my own, unaided work. It is being submitted for the Degree of Master of Science in the University of the Witwatersrand, Johannesburg. It has not been submitted before for any degree or examination in any other University.

_____

16th day of February 2005

Abstract

This report investigates the viability of satellite remote sensing in monitoring the rehabilitation of coal discard dumps. Four levels of thermal monitoring data were assessed in this project. These were: ground and below surface temperature probes; aerial thermal and atmospheric monitoring surveys; high altitude aircraft; and satellites.

Remote sensing methods measure only variation of temperatures on the surface of the dump. Fires on discard dumps are sub-surface fires, and the depth and extent of the fire below the surface cannot be easily inferred. The resolution of satellite sensors is a limiting factor for detecting individual hotspots on dumps. Small mine dumps occupy just a few pixels and the position of fires cannot be accurately assessed. Although the larger dumps are discernable, the variation of temperatures across the dump cannot be easily determined.

For the present, aircraft monitoring may be the most viable means of monitoring spontaneous combustion in coal discard dumps, until satellite resolutions improve further**.**

Table of Contents

DECLARATION 2

ABSTRACT 2

TABLE OF CONTENTS 2

LIST OF FIGURES 2

LIST OF TABLES 2

CHAPTER 1 INTRODUCTION 2

1.1 Background 2

1.2 Objectives 2

1.3 Report layout 2

CHAPTER 2 BACKGROUND 2

2.1 Coal in South Africa 2

2.2 Spontaneous combustion of coal 2

2.2.1 Factors affecting spontaneous combustion 2

2.3 Coal discard dumps 2

2.3.1 Mechanisms of oxygen ingress into coal discard dumps 2
2.3.2 Controlling spontaneous combustion on coal discard dumps 2
2.3.3 Case studies of coal discard dump rehabilitation 2

2.4 Fundamentals of remote sensing 2

2.4.1 Types of remote sensing systems 2
2.4.2 Types of sensors 2
2.4.3 Basic electromagnetic theory 2
2.4.4 Interactions with the atmosphere and the Earth's surface 2
2.4.5 A closer look at thermal remote sensing 2
2.4.6 Thermal imagery 2

CHAPTER 3 COAL FIRES AND REMOTE SENSING 2

3.1 Detection of coal fires 2

3.2 Identification of fire areas 2

3.3 Temperature conversion and sub-pixel temperature determination 2

3.4 The dual band method for short wave infrared bands 2

3.5 ASTER temperature and emissivity separation (TES) algorithm 2

3.6 Other applications of satellite remote sensing to mining 2

3.6.1 Mining Rehabilitation 2
3.6.2 Acid Mine Drainage 2

3.6.3 Regional monitoring 2
3.6.4 Use of radar imagery 2

CHAPTER 4 THE COMBUSION OF COAL DISCARD DUMPS IN SOUTH AFRICA 2

4.1 Background 2

4.1.1 Vryheid Coronation Colliery (VCC) 2
4.1.2 Durban Navigation Colliery (Durnacol) 2
4.1.3 Kleinkopje Colliery 2

4.2 Data Collection 2

4.2.1 Vryheid Coronation Colliery (VCC) 2
4.2.2 Durban Navigation Colliery (Durnacol) 2
4.2.3 Kleinkopje Colliery 2

4.3 Data processing 2

4.3.1 Vryheid Coronation Colliery (VCC) 2
4.3.2 Durban Navigation Colliery (Durnacol) 2
4.3.3 Kleinkopje Colliery, Witbank 2

CHAPTER 5 CONCLUSIONS 2

5.1 Conclusion 2

5.2 Further research 2

REFERENCES 2

APPENDIX 1: VRYHEID CORONATION COLLIERY DUMP NO.2 UNDERGROUND TEMPERATURE MONITORING DATA 2

List of Figures

Figure		Page
2.1	Wien's Displacement Law (Lillisand and Keifer, 2000).	23
4.1	Locality sketch showing the position of Vryheid Coronation Colliery.	36
4.2	Map showing layout of Vryheid Coronation Colliery	37
4.3	Extension of Dump No.2 by keying in material from Dump No.1 in compacted terraces.	37
4.4	Locality map showing the positions of Durnacol and VCC in northern Kwazulu-Natal.	39
4.5	Locality sketch of Durnacol indicating positions of the discard dumps.	40
4.6	Locality map showing the position of Kleinkopje Colliery.	41
4.7	Aerial photograph of Kleinkopje Colliery complex showing open pit and position of Landau II discard dump.	41
4.8	Positions of temperature probes on No.2 dump at VCC.	42
4.9	Aircraft monitoring flight line over Kleinkopje Colliery showing concentration of CO2 recorded on the flight.	46
4.10	Close up of light line over Landau II dump at Kleinkopje Colliery showing recorded CO2 concentrations.	46
4.11	Temperature variation with depth at all monitoring points in October 1995.	48
4.12	Monthly temperature variation with depth from October 1995 to June 2001 at B1/1.	49
4.13	Three month moving averages of variation of surface temperature with time at B1/1 and B1/3.	50
4.14	Variation of temperatures with depth in Dump 2 in October 1995.	51
4.15	Variation of temperatures with depth in Dump 2 in January 1999.	52
4.16	Aerial thermal survey of VCC Dump No.2 in October 1995.	53
4.17	Landsat 5 false colour composite and thermal infrared image of VCC for 1989.	55
4.18	Landsat 5 false colour composite and thermal infrared image of VCC for 1999.	55
4.19	Night-time airborne thermography images of Dump 3 at DNC, showing three views of the dump.	57
4.20	Night-time airborne thermography images of Dump 7 at DNC, showing three views of the dump.	58
4.21	Night-time airborne thermography images of Dump 8 at DNC, showing three views of the dump.	59
4.22	MAS 19-10-3 RGB composite of Durnacol discard dumps.	61
4.23	MAS first principle component image.	62
4.24	Aster Band 14 colour map.	63
4.25	Aster RGB 846 combination showing close ups of each of Dump 3, Dump 7 and Dump 8.	65
4.26	Map_SO2 ground temperature image.	66
4.27	A comparison of average concentrations of gases and small particulates inside and outside the smoke plume.	68
4.28	Percentage concentration change from upstream to inside of the plume.	69

List of Tables

Table		Page
2.1	Summarised results of oxygen concentrations through test soil covers (Bezuidenhout et al, 2000).	17
4.1	Landsat 5 detection bands.	43
4.2	Modis Airborne Simulator detection bands.	44
4.3	ASTER detection bands.	45
5.1	Comparison of the thermal data sets used in this project.	72

CHAPTER 1 INTRODUCTION

1.1 Background

The creative utilization of energy has quintessentially been the driving force of human progress. Fossil fuel reserves provide the majority of the global energy supply, with coal being an indispensable source for generations to come. Despite it's importance as a resource, coal mining is increasingly perceived as an unsightly and environmentally damaging practice.

Spontaneous combustion of discard dumps is a historical problem that has left a legacy of environmental degradation on many South African mines. As environmental legislation becomes more stringent, South African mining houses are forced to take more decisive steps in controlling and managing all sources of pollution on their mines.

Pollution from traditional coal discard dumps is a continuous threat to the receiving environment. Noxious gases such as carbon monoxide, sulphur dioxide and nitrogen oxides may be found in the surrounds of an active coal fire. The greenhouse gas, carbon dioxide, is emitted into the atmosphere. Water resources are threatened by acid mine drainage. Further pollution is caused by smoke and wind-blown ash, and general degradation results from damage to the surrounding ecosystems.

There is often uncertainty regarding the exact extent and size of the fire on the dump, making rehabilitation a very dangerous undertaking. The rehabilitation of waste dumps is also an expensive and technically challenging endeavour. Furthermore, the requirement of monitoring to be conducted for many years after final rehabilitation can prove to be an extremely costly long-term exercise, especially on abandoned mines.

The use of remote sensing techniques is becoming an increasingly valuable tool for us to check the impact of our activities on the environment at large. Satellites are a source of regular and consistent data that allows for the investigation of variables changing both spatially and temporally. With increasing competition and the concomitant reduction in cost, satellite derived remote sensing images are finding increasing application in mining.

This information could potentially provide the mining houses with a management tool that is not only cost effective, efficient and reliable, but also a regular means of monitoring potential fire areas and newly rehabilitated areas. The remote platform eliminates risks to the safety of mine personnel and allows for monitoring of

abandoned mines without incurring additional costs, since several monitoring variables can be assessed from a single satellite image. The potential for improved rehabilitation methods can also be effectively tested.

This investigation examines satellite remote sensing methods for the detection of fires on coal discard dumps. Two coalmines in northern Kwazulu-Natal were studied: Durban Navigation Colliery, near Dundee and Vryheid Coronation Colliery, in Vryheid. Several levels of remote sensing data have been used, from ground monitoring data, to low-level and high altitude aircraft to satellites. A comparison of these data sets allows for the determination of the level at which the fires are discernable, the ease with which they can be detected, and the practicability of satellite remote sensing in terms of data availability and cost.

The use of atmospheric monitoring as a remote sensing method is investigated at Kleinkopje Colliery. The detection of the gaseous combustion products gives indication of the presence of the coal fire.

It was found that satellite remote sensing does have potential to be a viable means of monitoring coal discard dumps for spontaneous combustion. However, application for monitoring on individual mines is limited by the coarse spatial resolution of the sensors used.

1.2 Objectives

To conduct an extensive literature review of the concepts of remote sensing and its application in fire detection

To determine if remote sensing, as a tool for fire detection on coal discard dumps, is applicable in the South African context.

Determine whether satellite data can be used as a simple and cost effective management tool to monitor rehabilitation on mines.

1.3 Report layout

The report begins with a background on the principles of spontaneous combustion of coal discards and satellite remote sensing. This is followed by a description of previous work, drawing on experiences of extensive surface and subterranean coal fires India and China. The sources and properties of remotely sensed data for three South African mines are presented. A critical evaluation of the applicability of remote sensing capabilities is carried out in terms of the stated objectives.

CHAPTER 2 BACKGROUND

2.1 Coal in South Africa

South Africa is the third biggest coal producer in the world. The recoverable coal reserves in South Africa amount to some 58 billion tons, equivalent to about l0 per cent of the world's total (this figure excludes low-grade, high-ash content coal which could add as much as 25 per cent to the country's total reserves) (Chamber of Mines, 2001). Most of South Africa's coal is of a bituminous thermal grade; only two per cent is anthracite, and 1,6 per cent coal of metallurgical quality (Chamber of Mines, 2001). At current production levels, coal reserves are estimated at 200 years (Chamber of Mines, 2001).

Coal must be screened and washed in order to meet the specifications of both the export and local markets. This results in large quantities of discard coal each year.

There are 19 coalfields in the country spread over an area of 700 kilometres from north to south and 500 km from east to west (Hocking, 1995). Generally the rank or carbon content of the coals increases eastwards while the number of seams and their thickness decrease (Hocking, 1995). Thus, Mpumalanga and Limpopo Province coals are usually classified as bituminous, occurring in seams up to several metres thick, while KwaZulu-Natal coals are often anthracitic and are found in relatively thin seams (Hocking, 1995).

The largest coal deposits are in the Highveld coalfields, where 5 major seams have been identified (Hocking, 1995). These extend to the Vryheid-Utrecht field of northern Natal. The Highveld seams, of which the Witbank area is the country's most productive, are thick horizontal formations with little variation (Hocking, 1995). In contrast, the same seams in northern Natal are bent and broken due not only to millions of years of geological upheavals but also to volcanic intrusions (Hocking, 1995). The Natal coals are therefore a lot more complex and have a higher rank.

2.2 Spontaneous combustion of coal

The propensity for coal to combust spontaneously lies in its ability to react with oxygen at ambient temperatures. This is an exothermic reaction. Combustion usually occurs when the rate of heat generation exceeds the rate of heat dissipation.

Spontaneous combustion is a historical problem on coalmines. Over the years, many theories have been developed to explain this phenomenon. These include (Wade, 1988):

- Pyrite theory: The oxidation of pyrite (FeS_2) is an exothermic reaction, which results in self-heating. However, this reaction is believed not to be causative unless pyrite is present in large quantities and in a finely divided state.

- Bacterial theory: Thought to be the cause of spontaneous combustion in hay, it has no real basis in coal.

- Heat of wetting of coal: Wetting coal generates heat, which increases the rate of oxidation. A 10˚C increase in temperature is known to double the rate of the oxidation reaction.

- Oxidation theory: This is the currently accepted theory on spontaneous combustion. The oxidation process occurs in four overlapping steps (Holding, 1994):

    i. Adsorption / chemisorption : Oxygen is adsorbed onto the surface of the coal and forms relatively unstable adsorption complexes which may decompose or react further. The formation of these complexes occurs predominantly at temperatures up to 70˚C, although it may continue occurring for the duration of the oxidation process. No CO is evolved during this stage.

    ii. Adsorption-complex decomposition: Decomposition of the adsorption complexes occurs and the weight of the coal decreases. This usually occurs at temperatures between 80˚C and 150˚C, though it may occur at temperatures as low as 35-40˚C. The decomposition of these complexes is oxygen independent and yields mainly CO.

    iii. Oxycoal formation: Chemical reactions occur which lead from the unstable adsorption/chemisorption complexes to the formation of stable oxygen-carbon complexes called oxy-coal. Reaction temperatures vary between 150˚C and 230˚C. These high temperatures are maintained by the high exothermicity of the oxycoal reactions. CO_2 is the dominant reaction product during this stage

    iv. Combustion: The formation of oxycoal ceases during this stage and coal combustion commences. Temperatures are typically in excess of 230˚C.

In theory, spontaneous combustion can occur wherever coal and oxygen come into contact. It can develop in oxygen concentrations of 10% and active heating may be sustained at levels as low as 6%. Smouldering combustion can be maintained at 2% oxygen levels.

2.2.1 Factors affecting spontaneous combustion

The following factors, were found to affect spontaneous combustion (Unal, 1995; Holding, 1994):

- Coal Rank: Rank refers to the degree of maturation or metamorphism achieved during the formation of the coal. As rank increases, the carbon content of the coal increases, and the volatile matter content, moisture content, oxygen content and internal surface area decreases.

- Temperature: The rate of oxidation increases with temperature. Additional exothermic reactions begin as the temperature rises, resulting in a further increase in the rate of heat generation.

- Oxygen Pressure: Oxidation rate increases with increasing oxygen partial pressure

- Particle Size: Since particle size relates to the surface area available to the reaction, the rate of oxidation usually increases with decreasing particle size. The internal surface area, described by the porosity, is also significant.

- Metal Sulphides: The heat generated by the oxidation of pyrites contributes to increased oxidation rates. The swelling of oxidized sulphides causes disintegration of the coal, increasing the surface area and creating more air pathways.

- Thermal Conductivity: A high thermal conductivity (determined by the overall thermal conductivity of the dump) implies fast movement of heat away from hot spots, and subsequent reduction in heat generation.

- Moisture: Adsorption of moisture by coal is an exothermic reaction. The amount of heat generated during oxidation is increased when there is a relative increase in atmospheric humidity to the vapour pressure exerted by the coal moisture. Conversely, the desorption of moisture is endothermic, resulting in a reduction of heat and retardation of oxidation.

2.3 Coal discard dumps

Discard dumps comprise of discard material from the processing plant and material excavated during mining. Raw coal is mined as a mixture of different sizes of coal and rock, which is cleaned and graded to a consistent quality suitable for specific markets. During this process, a large quantity of discard coal is produced. Discard

coal is usually of a low rank, making it more reactive and susceptible to spontaneous combustion.

South Africa produces an average of 239 million tons of coal per year, of which approximately 30% is discarded. This translates to an average of approximately 72 million tons of discards per year (South African Government, 2005).

A significant amount of energy is wasted by the disposal of fine discard coal (size less than 6mm) of saleable quality, due to undeveloped markets for it. In Germany, the percentage of combustible content in mine dumps is limited to 2% by regulation (Bassier *et al*, 2000).

Old discard dumps contain up to 20-30% coal (Bell *et al*, 2001). This, together with poor compaction associated with deposition by end tipping, which allows easy permeation of air and water, creates ideal conditions for spontaneous combustion to occur on discard dumps.

The oxidation of pyrite and organic sulphur in coal results in the production of sulphates and sulphuric acid that can be toxic to vegetation and results in acid water infiltrating surface and ground water resources. It also results in the generation of SO_2 upon heating. H_2S is formed as a product of incomplete oxidation. Other noxious gases emitted from burning spoils include CO and CO_2 (Bell *et al*, 2001).

In accordance with the Minerals and Petroleum Development Act (2002), mining houses are finding it increasingly difficult to obtain closure certificates and often remain liable for pollution problems long after mining operations have ceased. The South African Government (2005) has facilitated the implementation of its priority programmes, namely the strengthening of enforcement under MPRDA, identifying and managing mine pollution hot-spots, and the rehabilitation of abandoned and ownerless mines, with its Phephafso Strategy, which was developed by the Department of Minerals and Energy, in conjunction with the Council for Scientific and Industrial Research (CSIR).

Apart from the environmental degradation, discard dumps also form part of the social milieu on the mine, resulting in associated problems. Informal scavenging by neighbouring communities is a common problem. On one mine, a trespasser was found dead after huddling close to a crack on a discard dump to keep warm on a cold winters night. The emitted gases asphyxiated the man. Grazing cattle often hamper the growth of vegetation and disrupt the structural integrity of the cover.

2.3.1 Mechanisms of oxygen ingress into coal discard dumps

The availability of oxygen is an essential component for spontaneous combustion to occur. Eroglu (1999) found the following processes resulting in oxygen ingress into discard dumps:

- Natural Convection: As the air inside the heap is heated, it rises and is replaced by cold air from the outside. This circulation, also referred to as the chimney effect, supplies reactants to the dump and occurs only when the dump temperature is already higher than ambient. However, convection may also aid dissipation of heat from a hotspot.

- Wind Pressure: Wind blowing on the inclined faces of the dump causes the ingress of reactants into the dump.

- Molecular Diffusion: If there is a reaction of a gas component in the dump, then diffusion of that component will occur.

- Barometric Breathing: Changes in ambient pressure causes flow in and out of the dump.

- Thermal Breathing: Changes in ambient temperature induces flow through the dump.

- Oxygen ingress also depends on the particle size distribution, degree of water saturation and the degree of compaction of the material in the dump (Bell *et al*, 2001).

2.3.2 Controlling spontaneous combustion on coal discard dumps

There are a number of options available to deal with the problems presented by discard dumps. Some discard dumps contain a large percentage of saleable coal and re-mining may be economically viable. It was found that in the Witbank Highveld, approximately 60% of discards produced could be extracted for re-use (Grobelaar *et al*, 1995). This provides not only additional revenue for the mine, but also results in the removal of an unsightly problem and the gain of valuable land space.

Another option is to move the entire dump. There are, however, high costs associated with the transport of discard to a new site, compaction into a new dump, cladding and monitoring. The advantage is a carefully controlled and much safer dump area.

Liu *et al* (1997) describe the following methods in use in China:

- Digging: This entails digging deeply into burning layers and extinguishing the fire using a high-pressure water spray.
- Surface sealing, spraying and grouting: These attempt to seal the surface and thus isolate air inflow into the dump.
- Deep layer grouting: Described as the most commonly used and effective method, grouts of lime and clay are used to extinguish burning.
- Levelling and compressing: Equipment is used to level and compress the surface of the waste dump, thus isolating the air inflow paths to the burning layer.
- Controlled combustion: Wind pipes are inserted into the burning layer to enhance burning. The heat is collected for other uses, and the waste gases treated and released.
- Forming the dump in a layer-by-layer method, where a clay medium (up to 0.5 m depth) is placed between successive waste layers (up to 5 m depth).

Bassier *et al* (2000) report that in the Rűhr area in Germany, fires were successfully controlled and extinguished by:

- Water injection or surface watering
- Injection of filling materials or excavation of fire spots
- Coverage with inert materials
- Integration into a new waste dump.

There can be potential problems with using water extinguish coal fires. Carbon monoxide and hydrogen may be released from water-gas reactions with burning coal, resulting in a further rise in temperature (Bell *et al*, 2001).

The introduction of a cover layer is the preferred means of controlling spontaneous combustion on coal discard dumps in South Africa. Most commonly, any surface hotspots are excavated and allowed to cool before a capping layer, usually of compacted soil, is installed.

The main purpose of soil covers is to separate the waste from the surface environment, reduce the infiltration of water and to restrict the ingress of oxygen. Installation of a soil cover is often complicated by the danger due to internal instability of the dump structure and the presence of sinkholes. The degradation of covers could result in re-entry of oxygen and the subsequent re-ignition of fires.

The predominant problem associated with soil covers in South Africa is desiccation during dry seasons (Vermaak and Bezuidenhout, 2000), which is likely to be aggravated by elevated temperatures in the discard.

Cover systems can be grouped into soil, synthetic and composite covers. Soil covers are preferred largely due to the high cost associated with synthetic covers. Soil covers may be grouped into simple covers and complex covers. (Wates *et al*, 2000)

Simple covers usually comprise a single layer of fine textured soil. A high water content must be maintained in order to limit oxygen ingress. Seasonal variations in moisture results in desiccation cracking and degradation over time. These covers are usually more suitable for humid, high rainfall areas. In British Columbia, Canada, the minimum thickness required to maintain saturated conditions throughout the dry season is 2 m. (Wates *et al*, 2000)

Complex soil covers could comprise the following layers (Wates *et al*, 2000):

- Erosion control layer: Protects underlying layer, separates waste from burrowing animals and plant roots and stores water for evapotranspiration.
- Moisture retention zone: maintains constant moisture content in underlying barrier layer
- Upper drainage layer: prevents development of seepage forces and reduces hydraulic head on barrier layer
- Infiltration barrier: limits infiltration of water into underlying waste material
- Lower capillary barrier
- Basic layer.

The dominant method of oxygen transport through soil covers is the diffusion through partially gas-filled pores. (Vermaak and Bezuidenhout, 2000)

From the experimental work conducted by Bezuidenhout *et al* (2000), the multi-layer covered discard cells were more effective in reducing oxygen concentrations relative to single layer covered cells as seen in the **Table 2.1**. The table represents averaged oxygen concentrations (as %) over 10 seasons of monitoring.

Table 2.1 Summarised results of oxygen concentrations through test soil covers (Bezuidenhout *et al*, 2000).

Cover type	% Oxygen	
	Unvegetated	Vegetated
Uncovered	19	Not measured
Single Layer	5.4	6
Multi Layer	0.5	2.1

New discard dumps should be designed to mitigate the factors contributing to spontaneous burning. Design measures in use include (Bassier *et al*, 2000):

- Compaction of extensive heapings in the interior
- Avoidance of large surface areas for wind attack and wind channels
- Creation of slopes with gradients suitable for machine use
- Surface water management
- Disk-type layout and division using berms
- Separate dumping of different materials
- Low dumping heights to avoid natural demixing
- Inspection and monitoring.

2.3.3 Case studies of coal discard dump rehabilitation

Goldfields Greenside Colliery – Witbank

Described as 'South Africa's longest running dump fire' (SA Mining, Coal & Gold Base Minerals, 1994), the dump, lying adjacent to the N12 Johannesburg-Witbank highway, dates from 1946, when Greenside Colliery began operation. The objective of the R16-million encapsulation project was to place and compact coal discard within specifications laid down by the National Institute of Coal Research, thus preventing spontaneous combustion and preserving the coal portion of the discard; prevent the contamination of natural resources by runoff and seepage; and the covering of the old burning dump to prevent further combustion.

The project was conceived in three phases (Colliery Guardian, 1994):

Phase One: Half the burning dump from the highway side covered by 2000. This involved the use of 95 000 m^3 topsoil; 350 000 m^3 gravel (with equal amount of ash) and 4.9 million m^3 coal discard.

Phase Two: Covering the remainder of the burning dump by 2007. Anticipated use of 37 000 m^3 topsoil, 380 000 m^3 gravel (with equal amount of ash) and 4.9 million m^3 of coal discard.

Phase Three: Placing and compaction the remainder of the coal discard produced before mine closure. Estimated completion date 2014.

The dump will cover a total rehabilitation area of 64 hectares with a height of 60 m.

A layer of soft weathered sandstone gravel was placed on the dump to prevent the transmission of heat and covered with compacted coal discard. The gravel blanket was keyed into the burning dump as added security against slope failure. Ingress of oxygen was prevented by a 400 mm compacted topsoil barrier.

JCI Tavistock Colliery – Witbank

SA Mining, Coal & Gold Base Minerals (1992) describes a similar approach taken at JCI's Tavistock Colliery and South Witbank. The old dump was covered with 1 m compacted topsoil and a new dump built against this cover. It was believed that the cover would not only provide a shoulder for the new dump, but also prevent oxygen ingress and starve the smouldering discard coal in the old dump. Compacting the new dump will have the effect of further compacting the outer edges of the old dump.

Anglo Coal Springbok Colliery – Witbank

The Springbok Colliery rehabilitation was described by Garner *et al* (2001). Springbok Colliery was an underground bord-and-pillar operation and it operated in the sixties, seventies and early eighties. Discard materials were dumped in two major deposits - the "old" Springbok dump sited on the fringes of the Springbokspruit, and the "new" Springbok dump - sited upslope.

The discard material had a significant sulphur component, much of it pyritic, and accordingly all dumps generated large amounts of acidity. This resulted in a denuded and high acidic valley, with a stream running through it that contributed significantly to the pollution load entering the Olifants River.

Rehabilitation planning was tackled in two phases:

Phase 1: Rehabilitation of the valley and the old discard dump (1993 to 1994).

Phase 2: Rehabilitation of the "new" discard dumps and the associated "moonscape" areas (areas denuded of vegetation as a result of acid mine drainage) (1998).

In the process of reshaping the dump, extensive fires had to be extinguished. This was achieved by careful excavation of the burning area, followed by compaction of the residual material after cooling.

An inert layer at least 1 m thick (burnt ash or subsoil) was placed and compacted over the extinguished material to prevent any further spread of burning, and the dump was then reshaped to specification by adding more discard material on top of the inert layer.

Reshaping the dump was done by cut-to-fill techniques, and by the placement of the materials lifted from the Springbok valley. To minimise long-term erosion risks, the dump was "whale-backed", i.e. using a form without terraces.

The ideal system of dump covers is one in which water penetrates this surface readily (to support plant growth) but then does not readily penetrate into the underlying discard material. Bearing in mind the cost constraints of the Springbok Valley exercise, a 3-layer dump cover was designed for the Springbok dump:

Layer 1: 30 t/ha lime, spread evenly on top of the compacted discard. This is designed to intercept upward capillary movement of acid water, and to neutralise it so that the acidity does not destroy the ability of the overlying soil to support vegetation.

Layer 2: 250 mm of subsoil material (compacted to minimise air and water ingress).

Layer 3: 300 mm of good-quality topsoil, with minimum compaction, to ensure good plant growth.

This medium was then prepared for revegetation by extensive tillage and fertilisation. A "window" - without topsoil - was left on the back of the dump for the placement of waste from the "new" dump, when its rehabilitation began.

ISKOR Grootegeluk backfilling investigations

Farquharson *et al* (1992) reported on a large-scale test, which was conducted to determine the best practise for back-filling the pit. A 30 m deep box cut into the high wall of the opencast pit was filled with discard, and instrumented with thermocouples and gas sampling probes. Although the walls of the excavation on

three sides protect the material, ignition occurred after one year. The stages of development of spontaneous heating were apparent.

Initially, atmospheric concentrations of oxygen existed in the dump. Temperatures near the top rear, towards the high wall, were higher than atmospheric, and those near the bottom of the dump were below atmospheric. It was found that there was a complete air change in the dump in less than half an hour.

A pseudo-equilibrium condition was observed where temperatures at the top rear stabilised to just above 50ºC, temperatures at the toe followed atmospheric temperatures and oxygen levels reduced to about 15% concentration at the top rear of the dump. The top of the dump was moist.

These observations imply:

- Convective air flow – air entering at the toe and leaving through the top
- Oxygen is absorbed by the discard
- Moisture evaporates from the discard into the air stream
- Heat generated from the reaction was being carried out of the dump as sensible heat of the moist air.

After a year of this pseudo-equilibrium condition, ignition of the dump was indicated by negligible oxygen concentrations measured towards the top rear of the dump, and the release of combustion and pyrolysis products such as CO, CO_2, H_2, CH_4 and higher hydrocarbons. More than a month after ignition, thermocouple measurements had reached readings of over 400ºC. Only two months after ignition was smoke first seen emanating from the dump.

Although higher temperatures towards the top rear of the dump characterized the pseudo-equilibrium condition, the progression of the fires after ignition appeared to 'resemble a set of independent fires burning their own paths towards the places where air was entering the dump'.

Four months after ignition, the surface had become hazardous due to gas emissions and flames. Discard placed on the face of the burning heap ignited within days, and a 10 m layer of discard on top of a 1m sand cover began burning within a month.

2.4 Fundamentals of remote sensing

Various authors have defined remote sensing as the collection and interpretation of information about an object without being in physical contact with it. This broad definition could include measuring variations in force distributions (for example a gravity meter), acoustic wave distributions (for example sonar) and electromagnetic (EM) energy distributions (Harris, 1987).

For most environmental applications (as in this project), the focus is on acquiring data on how features on the Earth's surface emit and reflect electromagnetic energy. The analysis of these data yields important information about the object characteristics.

Within this context, a more specific definition is given by Harris (1987): "The acquisition of data and derivative information about objects or materials (targets) located at the Earth's surface or in its atmosphere by using sensors mounted on platforms located at a distance from the targets to make measurements (usually multispectral) of interactions between the targets and electromagnetic radiation."

There are several advantages to satellite remote sensing (Harris, 1987):

- Improved data coverage. Data can be collected from areas of limited accessibility.
- Homogeneity. Data may be acquired from one sensor on a particular satellite, which is spatially consistent.
- Data is spatially continuous and satellites provide large area coverage.
- Frequency of data collection is improved. Weather satellites can provide data every 30 minutes. TERRA (a NASA sun-synchronous satellite) passes the same point every 16 days.
- Data are in a format ready for computer processing.
- The time base of a single pass of a satellite is very restricted, so that spatial changes in environmental variables are minimized.
- Measurements are complementary to conventional observations.
- Cost savings.

Thus, new fires can be identified and the movement and spread of the fire can be assessed. However, a very significant disadvantage is the coarse spatial resolution of thermal channels on satellites. This makes small fires barely detectable.

2.4.1 Types of remote sensing systems

There are essentially two types of remote sensing systems, depending on the wavelength of energy used:

Active systems

In an active system, the instrument acts as both the source of energy and the detector of the returned energy – it generates its own energy and records the reflection of that energy back to the sensor. Active systems are low energy systems that operate in the long-wavelength microwave portion of the electromagnetic spectrum.

The most commonly used active remote sensing system is RADAR, which is an acronym for 'radio detection and ranging'. As the name suggests, radar systems use radio waves to detect and determine the distance of objects. The signal is emitted by the radar as a pulse. Earth features are discriminated by the strength and time of the return signal.

The major advantage of long wavelength systems is their ability to penetrate atmospheric interferences such as clouds, rain, haze and smoke. They are used predominantly for surface feature mapping, especially in areas that experience long term cloud cover.

Passive systems

Passive systems have an energy source that is external to the detector. The most common source is the sun. Passive systems are high-energy systems that operate in the shorter wavelengths of the electromagnetic spectrum. For most purposes this is the visible and infrared (near, middle and thermal) regions. Passive systems consist of:

- Reflected solar radiation sensors: These measure solar energy reflected back to the sensor, usually in the visible and near infrared regions.

- Thermal infrared sensors: These sensors record energy emitted by the Earth's surface. This energy consists of solar heating energy (short-wave solar energy that has been absorbed and re-radiated at longer wavelengths by the Earth's surface), geothermal energy, fires and human activities (for example steelworks).

2.4.2 Types of sensors

Framing systems

These are essentially camera systems that instantaneously acquire an image of an area. Vidicons follow the principle of a video recorder. An electrical beam passes

over the image recorded on a photosensitive surface and transmits it to a magnetic tape.

Scanning systems

Scanning systems consist of a detector that sweeps across an area. Electromagnetic energy radiated or reflected off the target hits the detector and is converted to an electrical signal. The signal varies with the strength of the energy received. The signal is then amplified and written to a tape, or transmitted to a ground receiving station. Most satellite sensors fall within this category.

Hyperspectral remote sensing

These instruments acquire images in many, very narrow spectral bands, typically of the order of 200 or more. Hyperspectral imaging allows for accurate characterisation of spectral reflectance curves. Thus, they allow the discrimination of features that differ within narrow bands that are often not distinguishable in coarser multispectral imagery.

2.4.3 Basic electromagnetic theory

All matter above absolute zero (0 K / -273˚C) emits electromagnetic radiation. The amount of energy radiated by a black body is a function of the temperature of the object, as shown in **Figure 2.1**.

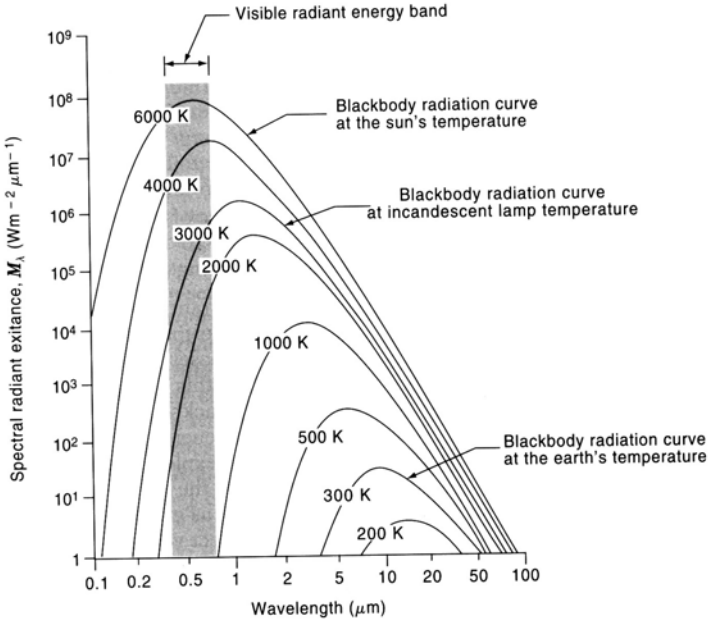

Figure 2.1 Wien's Displacement Law (Lillisand and Keifer, 2000).

As temperature increases, the total energy emitted by the object increases. The spectral distribution of energy emitted is also a function of temperature. As the

temperature of the object increases, the peak radiation emitted shifts to the shorter wavebands. A sensor working within the 3-5 μm window is very sensitive to detecting temperatures 600 K (327ºC) and above (surface fires), and sensors working in the 8-14 μm window detect objects with a temperature of 300 K (27ºC) (underground fires) (Zhang, 1998).

Usually, it is assumed that energy of wavelength less than 3μm is reflected (usually reflected solar energy). Energy emitted by ambient Earth features is of longer wavelength and is assumed to be greater than 3μm.

2.4.4 Interactions with the atmosphere and the Earth's surface

As the electromagnetic radiation interacts with the atmosphere in two ways (Lillisand and Keifer, 2000):

i. Scattering: The radiation is scattered by atmospheric gases and particles, which results in 'haze' in the imagery.

ii. Absorption: This implies effective loss of energy to atmospheric constituents (mainly CO_2, H_2O and O_3), which absorb specific wavelengths. Satellite sensors thus collect information in specific 'atmospheric windows', where the atmosphere allows transmission of energy.

Atmospheric constituents, both gases and aerosols, absorb radiation, thus reducing the apparent amount of energy emitted by the object, as detected by the sensor. Atmospheric particles also act as emitters themselves, contributing additional radiance to the signal detected by the sensor.

Therefore, atmospheric absorption and scattering make objects appear colder than they are. Conversely, atmospheric emission results in objects appearing warmer (Lillisand and Keifer, 2000). These effects are related to atmospheric path length (and vary with location, altitude, time of day and local weather conditions). It was found that temperature readings could be biased by as much as 2˚C at altitudes as low as 300 m (Lillisand and Keifer, 2000). Using air-to-ground correlation relationships, where a correlation relationship between scanner data and actual surface measurements is determined empirically, can compensate for these effects.

When incident EM energy encounters matter at the surface of the Earth, the three fundamental interactions that occur are reflection, absorption and transmission. The proportions of these interactions differ, depending on the type and condition of the material. These proportions also vary with wavelength.

This implies that we may be unable to distinguish one object from another in one wavelength band, but clearly distinguish between them in another spectral range. It is these characteristics that distinguish one object from another in remote sensing. The spectral response pattern is a spectral 'signature' for a particular object acquired over various wavelengths. (Lillisand and Keifer, 2000)

2.4.5 A closer look at thermal remote sensing

A distinction must be made between kinetic temperature and radiant temperature. Kinetic temperature may be regarded as an 'internal' manifestation which represents the 'average translational energy of molecules in a body' (Lillisand and Keiffer, 2000). Radiant temperature may be regarded as an 'external' manifestation of the energy state of the object (Lillisand and Keiffer, 2000). The object radiates energy as a function of its temperature

A blackbody radiates energy according to the Stefan-Boltzmann law:

$$M = \sigma.T^4$$

Where M= total radiant exitance from the material surface [W]; σ = Stefan-Boltzmann constant [5.6697x10-8W m^{-2} K^{-4}]; T = temperature of the blackbody [K].

The surface temperature is thus inferred from the radiant exitance, M, measured by the sensor over a discrete wavelength range. Real objects, however, do not behave as perfect blackbodies, so we introduce the concept of emissivity, ε, over a particular wavelength:

$$\varepsilon(\lambda) = \frac{\textit{radiant exitance of an object at a given temperature}}{\textit{radiant exitance of a blackbody at the same temperature}}$$

Emissivity varies with material type and condition, and wavelength, and has a numerical value between 0 and 1. The emissivity of a blackbody is 1. The emissivity of coal is approximately 0.95. For actual ground objects, the Stefan-Boltzmann law may be modified to include emissivity:

$$M = \varepsilon.\ \sigma.\ T^4$$

This implies that an object with high kinetic temperature may have low radiant temperature due to low emissivity.

For a blackbody, radiant temperature is equal to kinetic temperature. However, for real objects, the following relation applies:

$$T_{rad} = \varepsilon^{0.25}. T_{kin}.$$

Therefore, the radiant temperature measured by the sensor is less that the kinetic temperature of the object.

It must be noted that thermal sensors detect radiation strictly from the surface of the ground object only (they penetrate the surface only up to approximately the first 50 μm depth) (Lillisand and Keiffer, 2000).

2.4.6 Thermal imagery

The radiation received by the sensor is therefore a combination of surface temperature, surface thermal properties and atmospheric effects. Surface emissivity and atmospheric effects have to be corrected for in order to obtain reliable and accurate land surface temperatures. Zhang (1998) states that under clear atmospheric conditions, the atmospherically attenuated target radiance is compensated by path radiance emitted by the atmospheric constituents.

There is a diurnal variation in temperatures that must be borne in mind when dealing with thermal imagery. Pre-dawn or dusk time images are preferable since there exists a significant contrast between thermal anomalies and background areas.

In rugged terrain, topographic effects on solar heating substantially affects image brightness. Pre-dawn or nighttime imagery overcomes the problem of solar heating effects. Although reflected sunlight has no effect on the thermal channel, thermal shadows affect the clarity of the image.

In South Africa, north and northeast facing slopes tend to be warmer since they receive the most sunlight during the day. Coal dumps have low albedo and high thermal conductivity. They are efficient absorbers and emitters of solar radiation, resulting in the masking of deeper thermal radiation sources.

Also, winter images show more contrast than images taken in the summer months. Solar warming is reduced, and there is a more rapid loss of surface or near surface thermal radiation to the atmosphere due to the reduction in vegetation cover, cloud cover and atmospheric instability.

Using calibration relationships, scanner output values can be related to absolute ground temperatures.

CHAPTER 3 COAL FIRES AND REMOTE SENSING

Coal fires are a problem in many parts of the world. China is the world's largest producer of coal, with production in 2003 reaching a new record of 1 608 million tons (Mbendi, 2005). Fires consume, on average, 100 to 200 million tons per year (Van Genderen and Haiyan, 1997). China's coal reserves are widely distributed throughout the country. However, fires predominate over the north of the country, across a band of length 5000 km and width 450 km (Van Genderen and Haiyan, 1997).

The Jharia coalfields, the largest in India, are situated 250 km northwest of Calcutta (Prakash *et al*, 1997). The Jharia coalfield is the main source of prime coking coal in India.The area is littered with both surface and subsurface coal fires.

The large scale of the coal fire problems in India and China has resulted in extensive research programs to develop tools to detect the extent and severity of these fires. The fires in these countries span a regional scale and thus easily lend themselves to remote sensing methods. The studies conducted in both India and China are focused primarily on underground fires, their locations, temperatures and degree of spread. Remote sensing methods have proved invaluable in the study of underground coal fires over such a vast area, and in remote areas across mountains, deserts and other inhospitable terrain. Surface fires are also of concern, but occur to lesser degree.

Although the problem of spontaneously combusting coal reserves and discard dumps is prevalent on many South African mines, and the problem has been extensively researched, the incidence of these fires is localised to small areas on the scale of an individual mine.

3.1 Detection of coal fires

The aim of fire detection using remote sensing methods is to distinguish fire areas from their surrounds. Temperature measurements were carried out using boreholes until the first remote sensing coal fire study was conducted in Pennsylvania, USA in 1964 (Van Genderen and Haiyan, 1997). A thermal infrared scanner was flown aboard an aircraft to study fires on coal discard dumps.

Numerous data types may be used in coal fire detection:

i. Air photos and visible bands on satellite images may be used to detect smoke, the deposition of new materials on the surface (for example, sulphur deposits), and in the case of underground fires, change in colour of the cap rock and land cracking and subsidence.

ii. Infrared images: Short-wave infrared images are used to detect fires hotter than 160°C. Thermal infrared images are the most important in fire detection. Both day and nighttime images have been used, though nighttime images have the added advantage of eliminating solar heating effects.

The following satellite sensors have been used for fire detection (Van Genderen and Haiyan, 1997):

- LANDSAT TM band 6 (10 - 12.4 μm): Landsat 5 had a ground resolution of 120 m, which proved ineffectual for very small fires, but was used extensively in India (Prakash *et al*, 1997) and China. Landsat 7, with a resolution of 60 m, is now more widely used. The 16-day repeat cycle of Landsat, providing day- and night-time images, makes it ideal for routine monitoring of coal fire areas.

- NOAA - AVHRR: This platform was used extensively for forest fire and biomass burning applications. It has three thermal channels: Channel 3 (3.55 - 3.95 μm), Channel 4 (10.3 - 11.3μm) and Channel 5 (11.5 - 12.5μm). The spatial resolution is coarse at 1 km, but both day and nighttime images are available daily. It was used for the detection of underground fires in India, with some success (Prakash *et al*, 1997).

- ATSR ESA ERS-1: The use of this platform was somewhat unsuccessful in China, since the thermal band is centred at 11-12 μm and the spatial resolution is 1 km.

- SPOT XS: SPOT was found to be less useful than Landsat TM. SPOT XS has no thermal bands and a repeat cycle of 26 days.

iii. The analysis of atmospheric plumes from suspected fire areas also aids in fire detection. These can be conducted from aircraft or satellite sensors.

The pollutants emitted from combustion sources are carbon monoxide, sulphur oxides, nitrogen oxides, hydrogen chlorides, organic compounds, particulate matter and trace elements (Luckos, 2002). Approximately 99% of the carbon in the coal is converted to CO_2 during combustion. Particulate matter usually includes ash and unburned carbon particles from the incomplete combustion of the coal (US EPA, 1998).

Sulphur dioxide (SO_2) is the primary sulphur oxide produced, followed by much lower concentrations of sulphur trioxide (SO_3) and particulate sulphates (US EPA, 1998). Approximately 95 % of the sulphur in bituminous coal is

converted to SO_2 during combustion (US EPA, 1998). The sulphur oxides originate from the oxidation of the organic and pyretic sulphur in the coal during combustion (US EPA, 1998).

Nitrogen oxides consist mainly of nitric oxide (NO), with a small proportion of nitrogen dioxide (NO_2) (US EPA, 1998). A few parts per million of nitrous oxide (N_2O) is also produced (US EPA, 1998). The nitrogen oxides are formed from the oxidation of the nitrogen in the coal and the oxidation of atmospheric nitrogen in the combustion flame (US EPA, 1998).

Carbon dioxide (CO_2), methane (CH_4) and nitrous oxide (N_2O) are greenhouse gases. Both N_2O and CH_4 are formed from the incomplete combustion of the coal.

3.2 Identification of fire areas

A study conducted by Prakash *et al* (1997) compared the distribution of surface and subsurface fires across the Jharia coalfield. Short wave infrared (SWIR) images were used to study high temperature events in the range of 200°C - 1500°C. This would constitute Band TM5 (1.55 - 1.75 μm) in the Landsat TM platform used. Band TM6 (2.4 – 10.4 μm), the thermal channel, not only has a coarser resolution of 120 m, but also saturates at 68 C. It is therefore useful for detecting low temperature anomalies like underground fires, which manifest as surface temperatures of between 26°C and 32°C.

Anomalous pixels are identified by a combination of saturation in Band TM7 (2.08 – 2.35 μm) and no saturation in TM5. These pixels were found to have pixel integrated temperatures of between 344°C – 410°C. Anomalous pixels in TM5 that were not saturated in TM7 were found to range from 217°C – 276°C. Identification of surface fires is facilitated by a false colour composite (FCC) image with Bands TM7, TM5 and TM3 (0.63 – 0.69 μm) as RGB (Red Green Blue).

In another paper, Prakash *et al* (1995) describe processing techniques applied for the identification of underground fires. A non-linear stretched, density-sliced colour coded TM6 image was found to provide hue variations, but no information on relief, structure or topography of the surface. This image was then separated into its components of hue, intensity and saturation. A HIS (Hue Intensity Saturation) transform was applied to the image, where H was replaced with TM6, I replaced with TM4 and S with all pixels at a constant value of 255. In the resulting RGB image, pixels with successively higher temperatures were shown to vary from green

to yellow to red for the hottest pixels. The structural features of the surface were maintained in the background.

In Southern Africa, seasonal biomass burning is extensively practised. This has a direct impact on the ecological functioning, and distribution of biodiversity across these systems. Landman (2003) used Landsat ETM+ to quantify burn severity in the Kruger National Park. Pre-burn images were used to quantify available biomass using the Tasselled Cap reflectance.

Tasselled Cap is a transformation procedure similar to principal component analysis. The transformed axes represent: Brightness, which shows variation in soil reflection; Greenness, which represents the amount of vegetation in the scene; and Wetness, which relates to surface moisture (Lillesand and Keifer, 2000).

After controlled burning of the study areas, the Landsat ETM+ images were used to define the burn area, and predict the combustion completeness of each pixel, which is derived from the near infrared bands. The combustion completeness is determined by the change in reflection before and after the burn. A linear spectral unmixing model was used to separate the reflectance from the ash component of the pixel from the total pixel reflectance. A burn severity index was developed as a function of the ash abundance from spectral unmixing and the combustion completeness.

Landman (2003) found that burn severity depends more on the colour of the ash, which indicates efficiency of burning, than on the change in reflectance. This implies that for the same change in reflectance of the surface of a burned out area, there may be significant differences in the actual severity of the fire that occurred.

An audit of thermal remote sensing, with reference to applications in coalfield management, was conducted in South Africa by Harris (2001). The study focussed on the availability of nighttime imagery for fire detection. Nighttime imagery has the important benefit of greater thermal contrast due to reduced solar heating effects. Nighttime images from Landsat, ASTER and Talytherm were reviewed. Nighttime images from ASTER were available on request only and fires were usually too small to be effectively identified.

3.3 Temperature conversion and sub-pixel temperature determination

Digital numbers, representing the measured radiance at the sensor, must be converted to actual kinetic temperature of the object. This can be achieved for in three steps (Zhang and Kroonenberg, 1997):

i. Conversion of digital number to spectral radiance

ii. Conversion of spectral radiance to radiant temperature, using Plank's law

iii. Radiant temperature is converted to kinetic temperature assuming some emissivity for the ground material.

High temperature surface fires are usually smaller than the instantaneous field of view (IFOV) of the sensor. The pixel therefore represents a mixed signal from different proportions of fire and non-fire areas. The radiance received by the sensor is an average across the pixel.

Fires causing saturation of the pixel will be hotter than the measured temperature of the pixel. Thermal anomalies can be identified statistically as the sum of the statistical average of the pixels (which represents the background condition) and some multiple of the standard deviation (Zhang and Kroonenberg, 1997).

For Landsat 5, pixels values or digital numbers (DN), range from 0 to 255. This translates to a detection range of –69ºC to 68ºC for Band TM6. However, fires with temperatures greater than 68ºC occupying an area less than one pixel can be detected using this method if the pixel is not saturated, that is if the average temperature across the pixel is less than 68ºC. There is a combination of fire temperature and size that will produce an anomalous thermal pixel indicating a fire.

Zhang and Kroonenberg (1997) describe a method to determine the sub-pixel fire temperature for Landsat 5. The higher the background temperature, the more difficult it is to detect a fire. Also, large fires and fires with higher temperatures are easier to detect.

Zhang and Kroonenberg (1997) also found that Landsat 5 TM thermal data has too coarse a resolution for 'early detection of coal fires with a relatively small size and low temperature'.

3.4 The dual band method for short wave infrared bands

Prakash and Gupta (1999) investigated the use of Landsat TM short-wave infrared (SWIR) bands, TM5 (1.55 – 1.75 μm) and TM7 (2.08 – 2.35μm), to estimate temperatures of high temperature surface fires. According to Wein's Displacement Law, as shown in **Section 2.4.4**, as the temperature of the object increases, the peak radiation emitted shifts to the shorter wavebands. High temperature events, including volcanoes and fires, are therefore estimated using SWIR bands. TM5 and TM7 are together capable of measuring temperatures between 160˚C and 420˚C.

The method is not discussed in detail here, since fires on the discard dumps studied using Landsat do not reach such high temperatures on the surface. However, it was found that using the dual band method and data from TM5 and TM7, the subpixel area and subpixel temperature of the surface fires could be estimated. The method does have limitations and can be extended once more SWIR bands become available on newer satellites.

3.5 ASTER temperature and emissivity separation (TES) algorithm

ASTER has 5 thermal bands, as opposed to Landsat's one band. The conversion to surface temperature is therefore a complex procedure that involves an iterative procedure to integrate data from the five thermal bands and determine ground emissivities. ASTER is designed to develop a global emissivity map and recover surface temperatures. In order to achieve this the TES algorithm was developed.

For homogenous surfaces such as oceans, glaciers and forest canopies, the emissivity is known and the temperature can be easily determined. Yet, terrestrial pixels (90 m x 90 m) are composed of a number of different materials comprising of different temperatures and emissivities. The emissivities determined are thus integrated over the pixel.

The relationship between temperature and emissivity is non-deterministic. That is, there is an emissivity for each image band plus temperature and atmospheric parameters, which results in at least one extra degree of freedom (Gillespie *et al*, 1998).

The TES algorithm is an iterative, empirical procedure for determining the emissivity and temperature of individual pixels. It results in accuracies to within approximately 1.5 K for temperatures and 0.015 for emissivities (Gillespie *et al*, 1998). The TES algorithm is used to create the ASTER temperature and emissivity data products.

3.6 Other applications of satellite remote sensing to mining

Satellite remote sensing is finding increasing application in the mining industry, particularly in the field of monitoring the impact of mining and rehabilitation measures. However, it has been found consistently that the potential for local scale monitoring is limited by satellite spatial, and to some extent spectral, resolution.

On regional scale analysis, however, its application has proved to be particularly useful, not just for governments, but also for mining houses that have operations spread over large areas. Satellite remote sensing could prove to be more cost

effective, especially in inaccessible areas, where monitoring would otherwise have to be done by helicopter or high-resolution aerial photography. A few cases of satellite remote sensing in mining applications are given below.

3.6.1 Mining Rehabilitation

A study conducted by Limpitlaw *et al* (2000) at Vryheid Coronation Colliery used Landsat TM images to test the effectiveness of rehabilitation efforts on the mine. Three scenes were acquired spanning a 10-year period to compare the detectable change in environment. A normalised difference vegetation index (NDVI) was used to delineate areas of strong vegetation response. The resulting colour composite image showed trends in vegetation cover over the study period.

A supervised classification was attempted to automatically identify areas affected by mining, such as newly disturbed areas, disturbed but subsequently rehabilitated areas and unchanged areas. This technique was found to work over large homogenous areas, but was less successful for small areas such as pits, that cover only 1 or 2 pixels.

It was found that although the medium resolution of Landsat was sufficient to provide information on rehabilitation progress over time, the resolution was too coarse for small changes, such as the early stages of gully development. It was recommended that medium resolution satellite imagery be used in conjunction with conventional monitoring techniques, though the frequency of those can be substantially reduced.

3.6.2 Acid Mine Drainage

Anderson and Robbins (1998) used airborne digital multispectral video to detect iron oxide precipitates associated with acid mine drainage. Although satellite imagery was found to be good for wide, higher order streams, its spectral and spatial resolution is poor for smaller headwater streams.

They found that in the 650 – 750 nm wavelength region (red to near IR), acid precipitates had higher spectral reflectance than neutral iron rich streams. Clean, unimpaired streams were found to have no reflectance in this wavelength range.

Algal pigment contributions to spectral signature are significant depending on the type of acid mine drainage and the characteristics of the stream. It was thus concluded that a suite of detection strategies be adopted for different types of acid mine drainage.

3.6.3 Regional monitoring

Coal and uranium mining in the former German Democratic Republic caused extensive environmental degradation. Böhm *et al* (2000) describe the programme implemented to monitor rehabilitation efforts. Remotely sensed data was used to assess:

- Soil and rock chemistry and identification of pollution and toxic soils
- Land cover and vegetation type
- Monitoring changes in vegetation and soil moisture to identify contaminated runoff
- Monitoring rehabilitation work and its success
- Thematic maps for the planning of recultivation and rebuilding of infrastructure
- Three-dimensional observation to detect mass movements in early stages to take precautionary measures.

Space-borne remote sensing instruments used were IRS 1C, Landsat TM and ERS 1 & 2 Synthetic Aperture Radar. Airborne high-resolution imagery was used in conjunction with the satellite data. The ground resolution of satellite imagery was a limiting factor, as well as cloud cover affecting repetition times. However it was found to be a fast and cost effective means of getting an overview of large scale mining areas.

In the West Rand, Gauteng, Chevrel and Coetzee (2000) used satellite data from SPOT and Landsat TM to compile inventories of polluted areas, define areas that are susceptible to pollution and identify pollution dispersal pathways. The following factors were mapped:

- A land cover map providing accurate classification of mining areas and potential pollution sources
- A linear-feature density map derived from linear discontinuities observed on images, representing fracture density
- A surface run-off and drainage pattern map derived from flow accumulation algorithms applied to digital elevation models
- A GIS system was developed to create risk/sensitivity maps.

3.6.4 Use of radar imagery

Master and Woldai (2001) used multi-temporal ERS-1 synthetic aperture radar to distinguish between slimes dams, waste and slag dumps due to differences in radar reflectivity in copper mining areas of the Democratic Republic of Congo. Polluted areas appeared dark due to the absence of vegetation. Multi-temporal imagery was used to define present drainage lines and seasonally differing soil moisture zones. The work demonstrated the use of remote sensing data in areas that are inaccessible due to physical remoteness or political instability.

CHAPTER 4 THE COMBUSION OF COAL DISCARD DUMPS IN SOUTH AFRICA

Three sites were investigated where there was a historical problem of fires on discard dumps. Two sites were investigated using satellite remote sensing methods. These are the Vryheid Coronation Colliery and Durban Navigation Colliery sites. Rehabilitation efforts were either complete or in progress at these sites. The third site, at Kleinkopje Colliery, was investigated using atmospheric monitoring methods.

An attempt was made at obtaining several levels of remote sensing data (ground data, aircraft, high-altitude aircraft and satellite) for the same time frames. This would enable direct comparison. However, data of this nature were unavailable and the analysis was based on whatever data sets were available at the time.

4.1 Background

4.1.1 Vryheid Coronation Colliery (VCC)

VCC is found northeast of the town of Vryheid in northern Kwazulu-Natal (**Figure 4.1**). The coal seams were found in layers penetrating through the hills and were mined through by board and pillar methods. The pillars were later robbed, resulting in subsidence of the natural hills. The mine was closed in 1993.

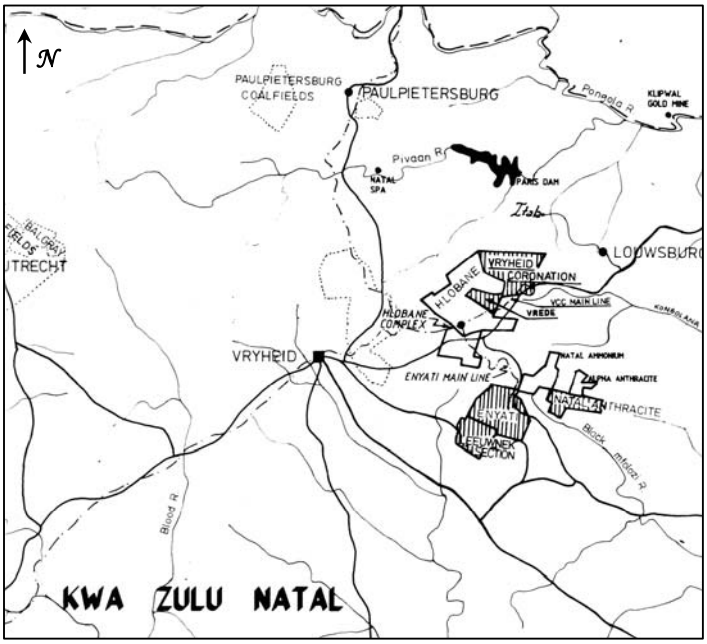

Figure 4.1 Locality sketch showing the position of Vryheid Coronation Colliery.

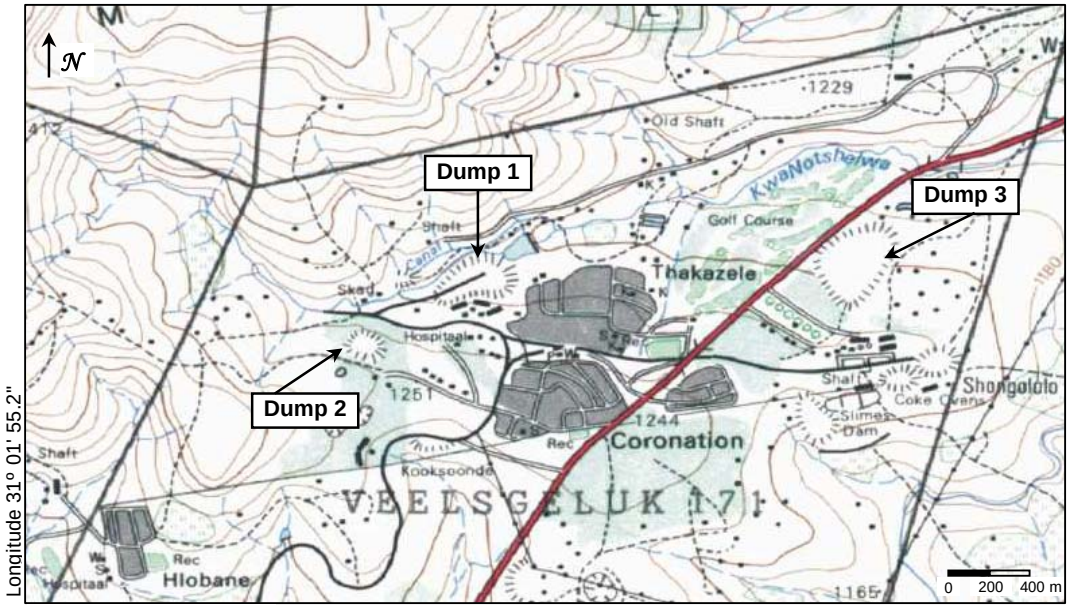

Figure 4.2 Map showing layout of Vryheid Coronation Colliery.

There were originally three discard dumps created on the mine, as shown in **Figure 4.2**. The No.1 dump was started in 1920, in the early days of mining at VCC. Between 1990 and 1995, the dump was successfully re-mined and the remaining discard used to extend dump No.2. The burning material was cooled and then compacted into terraces at dump No.2. Between 1998 and 1999, No.1 dump was reshaped and vegetated to its existing form.

Figure 4.3 Extension of Dump No.2 by keying in material from Dump No.1 in compacted terraces.

No.2 dump was started in approximately 1940, and was used up to the 1980s, when No.3 dump was started. The No.2 dump lies above an undermined area. Consequently, water percolating through the dump drains into the collapsed workings below.

Spontaneous combustion was experienced on No.1 and No.2 dumps for many years. Dumping was carried out by means of a rope carriage system, where filled carts were tipped and returned to the workings. This had resulted in uncompacted heaps open to oxygen ingress and subsequent fires.

Fires were reported by mine personnel on both these dumps a few years after inception. Cracks larger than 10 cm appeared and sulphurous smoke emanated from the dumps. In 1983, a fatality occurred when an elderly man seeking warmth went to sleep beside a crack on the dump. He was poisoned by the CO released. In the early 1980s burnt ash near the bottom of the dumps was mined for road construction.

The rehabilitation of Dump No.2 was completed by February 1995, using a 0.5 m layer of topsoil and vegetated to a final rehabilitated area of 13 ha. Re-levelling of the top of the dump took place in May 2000 to improve drainage. Temperature probes were installed by October 1995 and thermal imagery taken. In order to maintain the integrity of the cover at closure, bird perches were placed to encourage birds of prey to control burrowing animals, and a member of the local community was employed to stop cattle from straying onto the dump.

4.1.2 Durban Navigation Colliery (Durnacol)

The rich history of Durnacol is recounted in the book by Hocking (1995). In spite of its name, Durban Navigation Collieries (Durnacol) is sited between Dundee and Newcastle in northern Kwazulu-Natal **(Figure 4.4)**. The area once supported numerous coalmines to supply the steamship industry. The discovery of Durnacol coal's coking properties for steel production let to its becoming a subsidiary of ISKOR, the national steel manufacturer, in 1954.

Durnacol enjoys a colourful history as one of the most innovative mines in its almost 100 years of operation. Founded in 1903, the region is both geologically and chemically challenging. The area is straddled with convoluted coal strata frequently interrupted by dolerite or sandstone. Methane occurs in hazardous concentrations. A large underground explosion occurred in 1926, which left 126 fatalities.

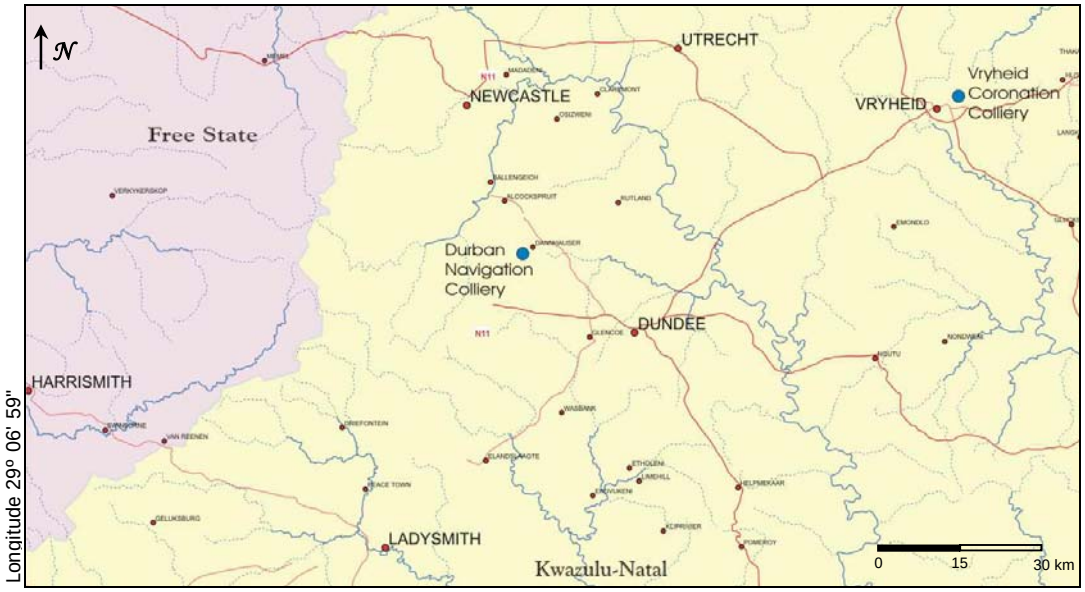

Figure 4.4 Locality map showing the positions of Durnacol and VCC in northern Kwazulu-Natal.

The Dannhauser dolerite contains iron pyrites, which adds to the coal's sulphur content, thereby increasing its acid potential and its susceptibility to spontaneous combustion.

Spontaneous combustion of the waste dumps at Durnacol is not a recent problem. In the 1980's record was made of No.1 dump being the only one not burning (the most recent dump at that time being No.7). In the eighties, No.3 dump was regarded as a nuisance, "in that every time the wind blew there was a cloud of black dust. Ash had been piled at the toe of the dump in an effort to reduce oxygen ingress" (Hocking, 1995).

Further efforts to rehabilitate the dumps took place in the late 1980s. "Those at No.1 and No.2 now boasted trees, shrubs and grass which made them look natural. As yet the No.3 dump remained stark and daunting, but in time that too would be compacted and improved" (Hocking, 1995).

Dumps 3, 7 and 8 are studied in detail for detection of fires. The positions of these dumps are indicated on **Figure 4.5**. Airborne thermographic images were available for these dumps. Dump No.8 is in the process of being rehabilitated. Dump No.7 and 8 have active fires and rehabilitation of these is in the design phase.

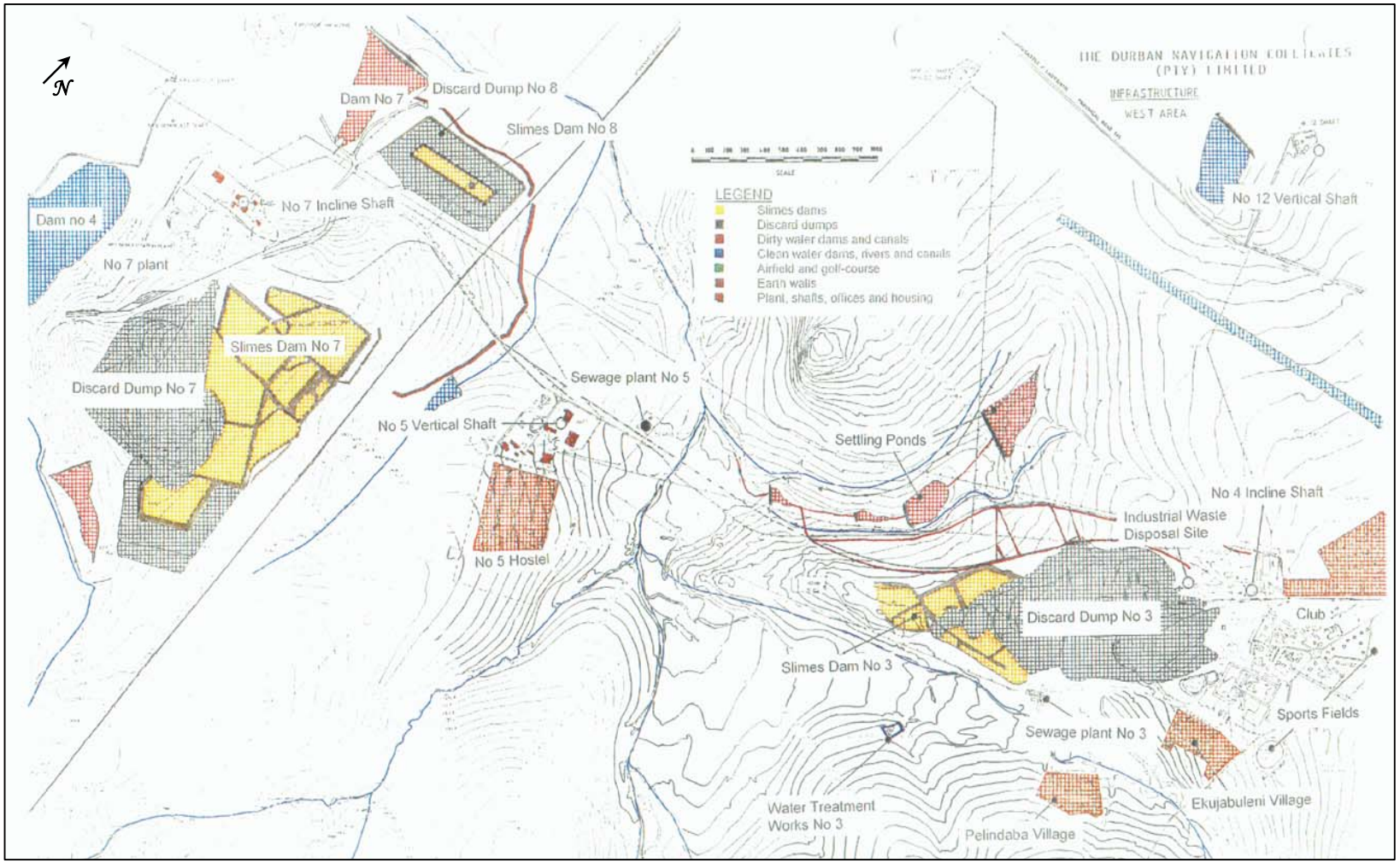

Figure 4.5 Locality sketch of Durnacol, obtained from mine records, indicating positions of the discard dumps.

4.1.3 Kleinkopje Colliery

Klienkopje Colliery is an opencast coalmine situated 10 km south of the town of Witbank, in Mpumalanga province **(Figure 4.6)**. The Nos.5, 4, 2 and 1 seam reserves being mined have previously been mined to varying degrees by underground bord and pillar methods. The current opencast mining results in the removal of all remaining coal, including coal in the roof and pillars of the old underground workings.

The Landau II dump consists of material that has not been compacted. The dump is not covered and rehabilitated, and ponding of stormwater on the top of the dump results from inadequate drainage. The Landau II dump is burning on the southwestern side. Step failures of the slopes on this side are also evident. The historical fire problem on the dump can be attributed to the prevailing wind direction and the lack of compaction and drainage of the dump.

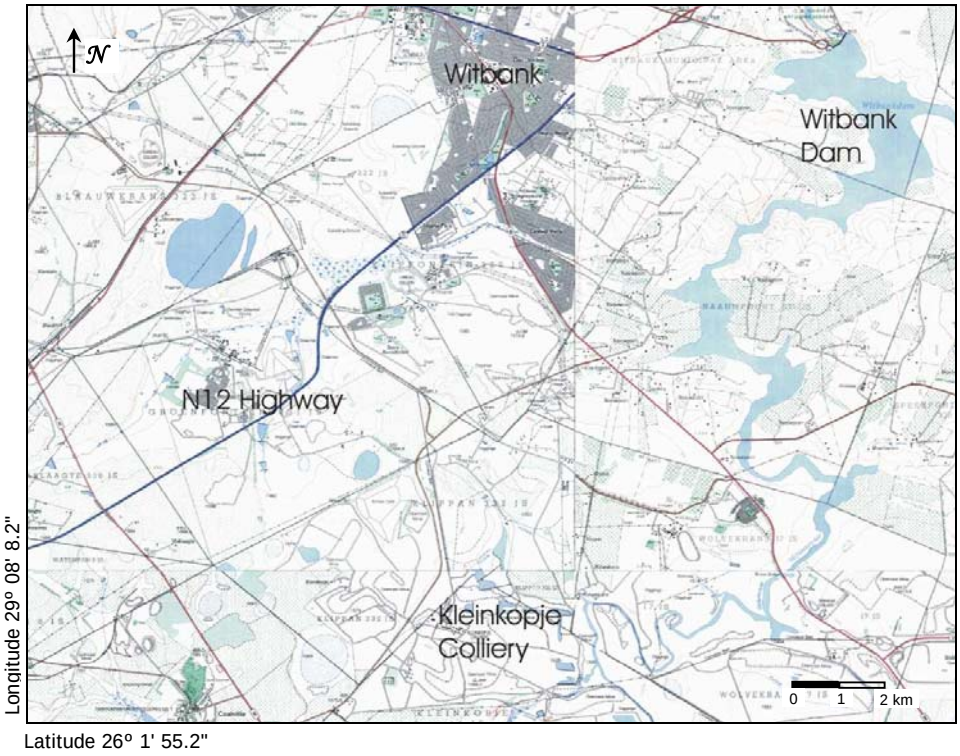

Figure 4.6 Locality map showing the position of Kleinkopje Colliery.

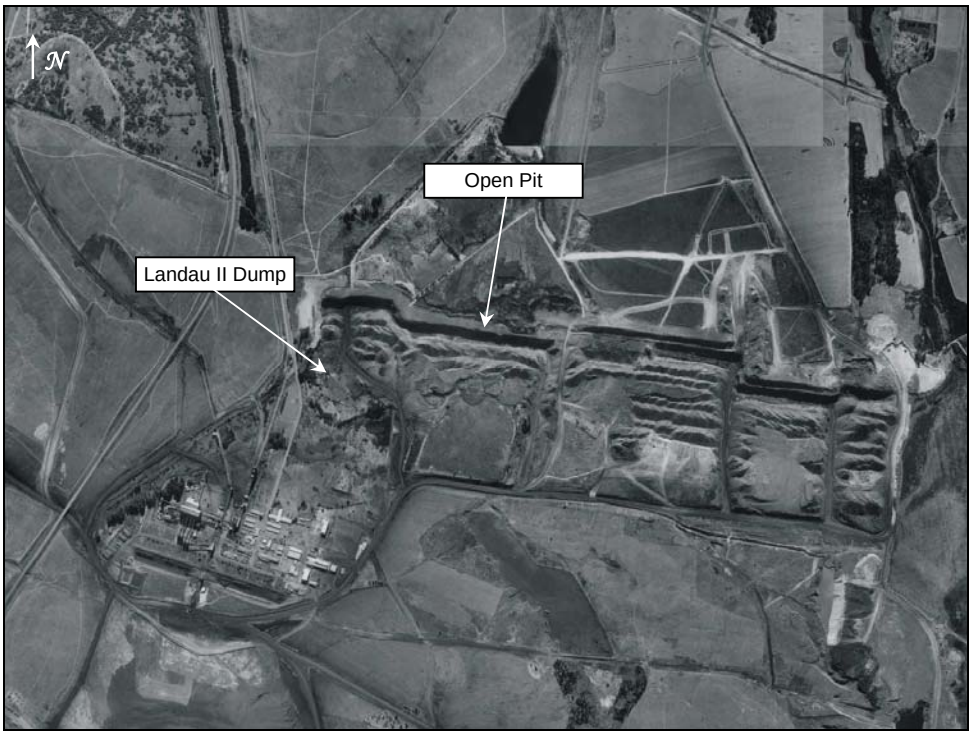

Figure 4.7 Aerial photograph of Kleinkopje Colliery complex showing open pit and position of Landau II discard dump.

4.2 Data Collection

4.2.1 Vryheid Coronation Colliery (VCC)

Ground monitoring data

In October 1995, eight temperature probes were placed on the northern end of dump No.2. These consisted of 6 m gun barrels placed vertically into the dump (top and first bench) and horizontally into the terrace of the dump (third bench), as indicated on **Figure 4.8**. The south side of the dump was cool, probably due to the effects of the dominant wind in the area. Readings were taken monthly, at 0.5 m depth intervals. Extra monitoring points were placed on benches 4, 5 and 6, between July and August 2000, to investigate a suspected hot spot.

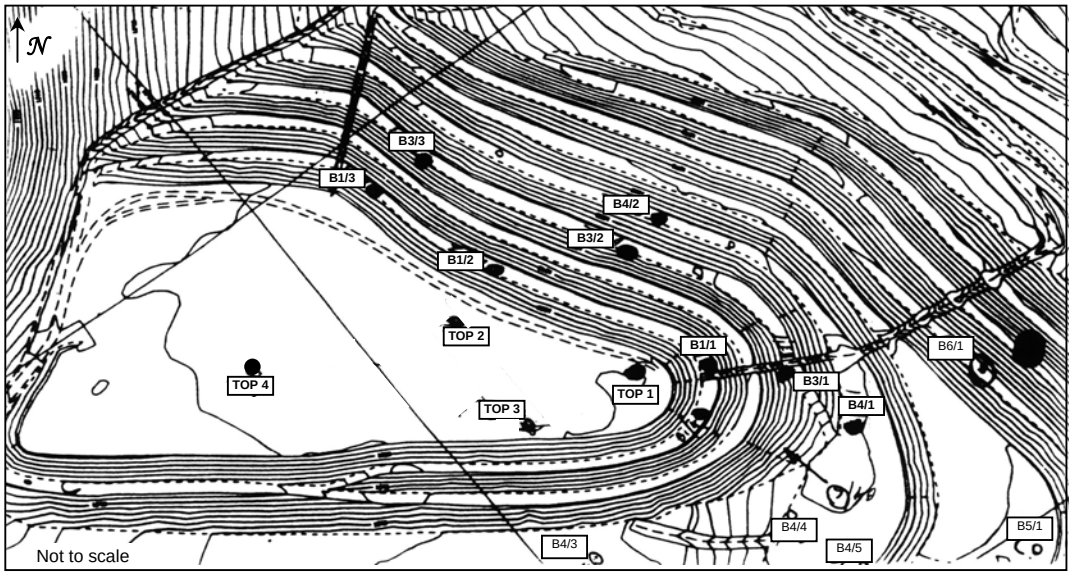

Figure 4.8 Positions of temperature probes on No.2 dump at VCC.

Aircraft data

In 1995, after rehabilitation of Dump No.2, nighttime aircraft thermography was conducted by the mine to inspect the thermal status of the dump. An Aga-450 Thermal Imager was flown aboard a helicopter at an altitude of approximately 10 000 ft (3 048 m). This resulted in a pixel size of approximately 0.5 m.

Satellite data

Landsat 5 was launched in 1984. It is a polar orbiting satellite, orbiting at an altitude of 705 km. It collects data along a swath of 185 km and has a revisits frequency of 16 days. Landsat 5 Thematic Mapper (TM) images of the mine were available for 3 April 1989 and 9 January 1999, taken at approximately 10:00 am. These sub-scenes cover an area of 25 x 25 km. The data consist of 7 bands, as described in **Table 4.1.**

Table 4.1 Landsat 5 detection bands.

Band number	Wavelength range (µm)	Description	Ground resolution (m)
TM 1	0.45 – 0.52	Blue	30 x 30
TM 2	0.52 – 0.60	Green	30 x 30
TM 3	0.63 – 0.69	Red	30 x 30
TM 4	0.76 – 0.90	Near Infrared	30 x 30
TM 5	1.55 – 1.75	Short Wave Infrared (SWIR)	30 x 30
TM 6	10.4 – 2.4	Thermal infrared (TIR)	120 x 120
TM 7	2.08 – 2.35	Short Wave Infrared (SWIR)	30 x 30

4.2.2 Durban Navigation Colliery (Durnacol)

Aircraft

A nighttime thermal aerial survey by helicopter was conducted on 3 March 2000 at approximately 9:00 pm, to monitor spontaneous combustion on the dumps.

High altitude aircraft

The Modis Airborne Simulator (MAS) is a scanning spectrometer flown aboard NASA's ER-2 high altitude research aircraft. Flying at an altitude of 20 km, images are obtained at a ground resolution of 50 m, over a 50 band spectral range. The fifty bands are given in **Table 4.2**. The thermal bands are from Band 26 to Band 50.

The image was taken on the 22 August 2000, Flight number 00-149, as part of the SAFARI 2000 campaign. Safari 2000 is an initiative between South African scientists and NASA to validate, by ground truthing, the data produced by the ASTER and MODIS instruments aboard NASA's TERRA satellite. The ER-2 is a research aircraft that carries airborne versions of the instruments aboard the satellite. These are used for the validation and calibration of the instruments aboard the satellite. The aircraft flew over areas of particular significance to researchers. This data is not available commercially.

Table 4.2 Modis Airborne Simulator detection bands.

Band	Spectral range (µm)	Band	Spectral range (µm)	Band	Spectral range (µm)
1	0.4451-0.4848	18	2.0309-2.0793	35	4.4648-4.6160
2	0.5285-0.5703	19	2.0794-2.1280	36	4.6184-4.7775
3	0.6294-0.6805	20	2.1291-2.1774	37	4.7778-4.9294
4	0.6816-0.7231	21	2.1779-2.2259	38	4.9298-5.0767
5	0.7221-0.7641	22	2.2278-2.2675	39	5.0888-5.2288
6	0.8034-0.8461	23	2.2777-2.3265	40	5.2412-5.3738
7	0.8460-0.8874	24	2.3274-2.3750	41	5.3590-5.4365
8	0.8867-0.9276	25	2.3764-2.4246	42	8.3391-8.7341
9	0.9277-0.9674	26	3.0384-3.2000	43	9.4541-9.9906
10	1.6163-1.6682	27	3.2066-3.3552	44	10.278-10.736
11	1.6722-1.7228	28	3.3521-3.5138	45	10.776-11.247
12	1.7245-1.7752	29	3.5170-3.6709	46	11.776-12.196
13	1.7768-1.8259	30	3.6724-3.8174	47	12.713-13.089
14	1.8303-1.8792	31	3.8267-3.9870	48	13.041-13.500
15	1.8801-1.9288	32	3.9929-4.1484	49	13.540-14.075
16	1.9312-1.9794	33	4.1365-4.2034	50	14.051-14.428
17	1.9804-2.0291	34	4.3401-4.4656		

Satellite

The Advanced Spaceborne Thermal Emission and Reflection Radiometer (ASTER) was launched on board NASA's Terra satellite in December 1999. It consists of 14 bands, as described in **Table 4.3**. Each scene covers an area of 60 x 60 km. A level

1B image, which is radiometrically and geometrically corrected, was acquired for the 28 December 2000 at 10:26 am.

Table 4.3 ASTER detection bands.

Band No.	Spectral Range (μm)	Subsystem	Spatial Resolution, m
1	0.52-0.60	VNIR	15
2	0.63-0.69		
3N	0.78-0.86		
3B	0.78-0.86*		
4	1.60-1.70	SWIR	30
5	2.145-2.185		
6	2.185-2.225		
7	2.235-2.285		
8	2.295-2.365		
9	2.360-2.430		
10	8.125-8.475	TIR	90
11	8.475-8.825		
12	8.925-9.275		
13	10.25-10.95		
14	10.95-11.65		

* *Back looking for stereo coverage*

4.2.3 Kleinkopje Colliery

An aircraft monitoring flight was conducted over the discard dump on 3 September 2003 to measure gas emissions over the dump. The plume, approximately 400 m long, was detected spreading to the east of the dump. The aircraft flight line is shown in **Figure 4.9**.

The aircraft made three passes over the dump. The close up of the flight line over the dump can be seen in **Figure 4.10**.

The data collected by the aircraft was calibrated for pressure and altitude. Data was collected for CO, NO, SO_2, O_3, NO_2, NO_x, CO_2 and particulates of the size range 0.1 μm to 3 μm.

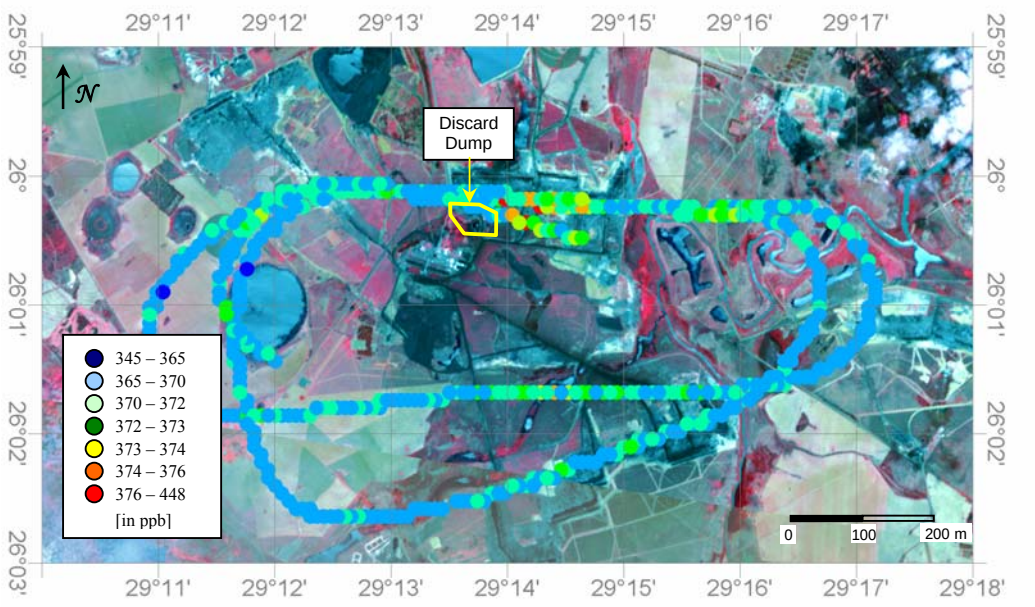

Figure 4.9 Aircraft monitoring flight line over Kleinkopje Colliery showing concentration of CO_2 recorded on the flight.

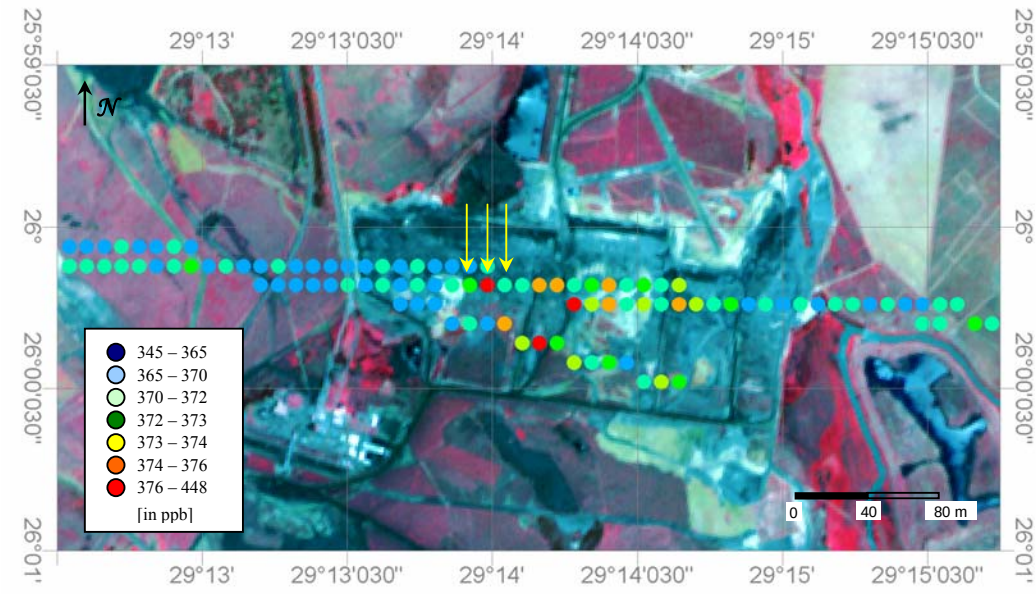

Figure 4.10 Close up of light line over Landau II dump at Kleinkopje Colliery showing recorded CO_2 concentrations.

4.3 Data processing

4.3.1 Vryheid Coronation Colliery (VCC)

Ground monitoring data

All borehole monitoring data of temperatures collected between October 1995 and June 2001 is given in Appendix 1. The variation of temperature with depth at each of the points is given in **Figure 4.11**.

A hot spot was identified on Bench 1 at point B1/1, where the dump was extended. It is believed that the interface between the two materials was not adequately compacted and keyed in, resulting in a zone of greater permeability. This enhanced oxygen ingress and accelerated spontaneous combustion.

The variation of temperature with depth over the monitoring period (October 1995 – June 2001) at B1/1 is shown in **Figure 4.12**. Temperatures in excess of 300°C are evident at 6 m vertically below point B1/1. The temperatures follow the same pattern of variation through the depths, except between 3 m and 4 m, where they generally remain consistent at around 97°C. A change in material, with a different heat capacity, dumped at that depth might result in this type of behaviour. A drop in temperature occurred in 2000, when rehabilitation work was done on the dump.

The hotspot below the surface does manifest as an increase in temperature at the surface. B1/3 lies on the same contour on the northern slope as B1/1 and displays no evidence of a fire below it. The surface temperature at this point may be regarded as ambient. The monthly surface temperatures at these two points, smoothed using a three point moving average, are plotted on **Figure 4.13**.

The plot shows consistent seasonality, with higher temperatures reported in summer. Both graphs follow the same trend. A t-test was conducted to determine if there was a significant difference between the two data sets. The probability that the two samples came from the same population was 0.00163. This implies that there is a significant difference between them at more than a 99 % level of confidence. On average, the surface temperature at B1/1 is 4°C higher than the ambient conditions defined by B1/3.

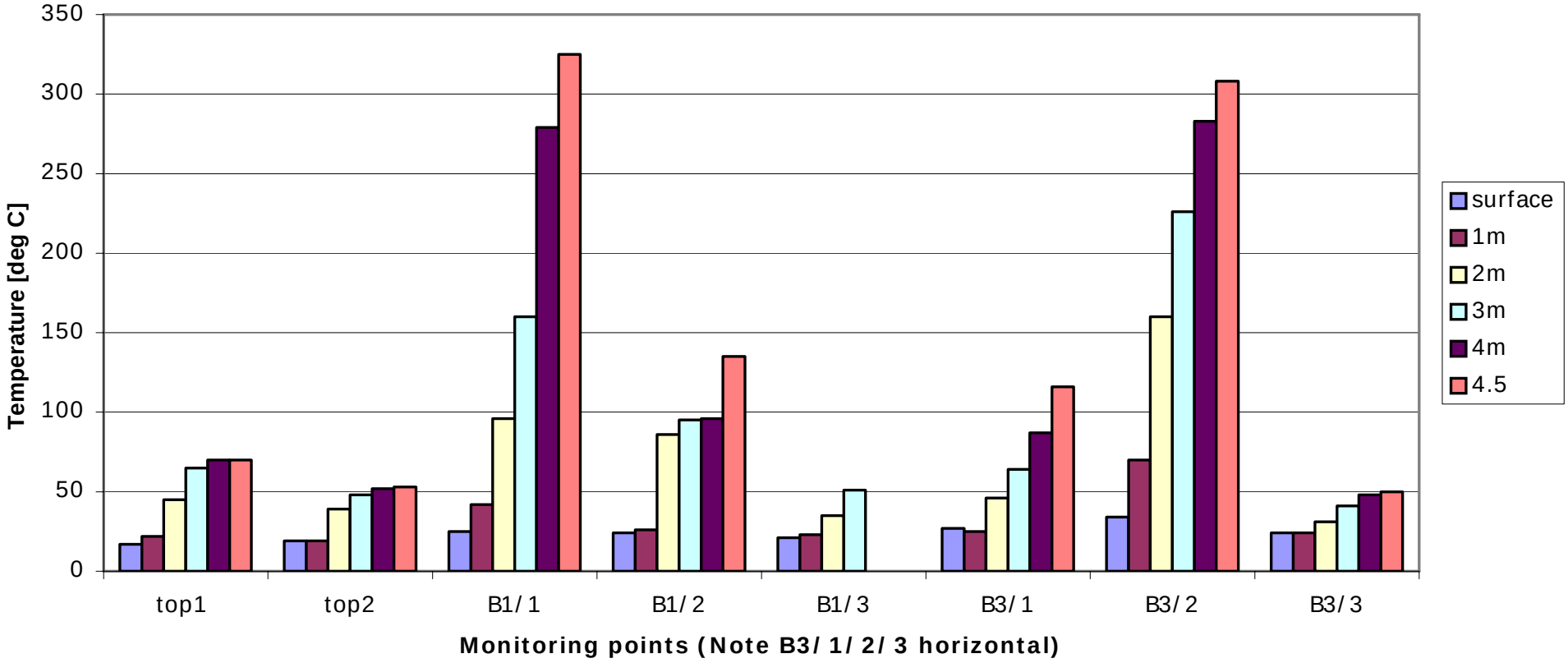

Figure 4.11 Temperature variation with depth at all monitoring points in October 1995.

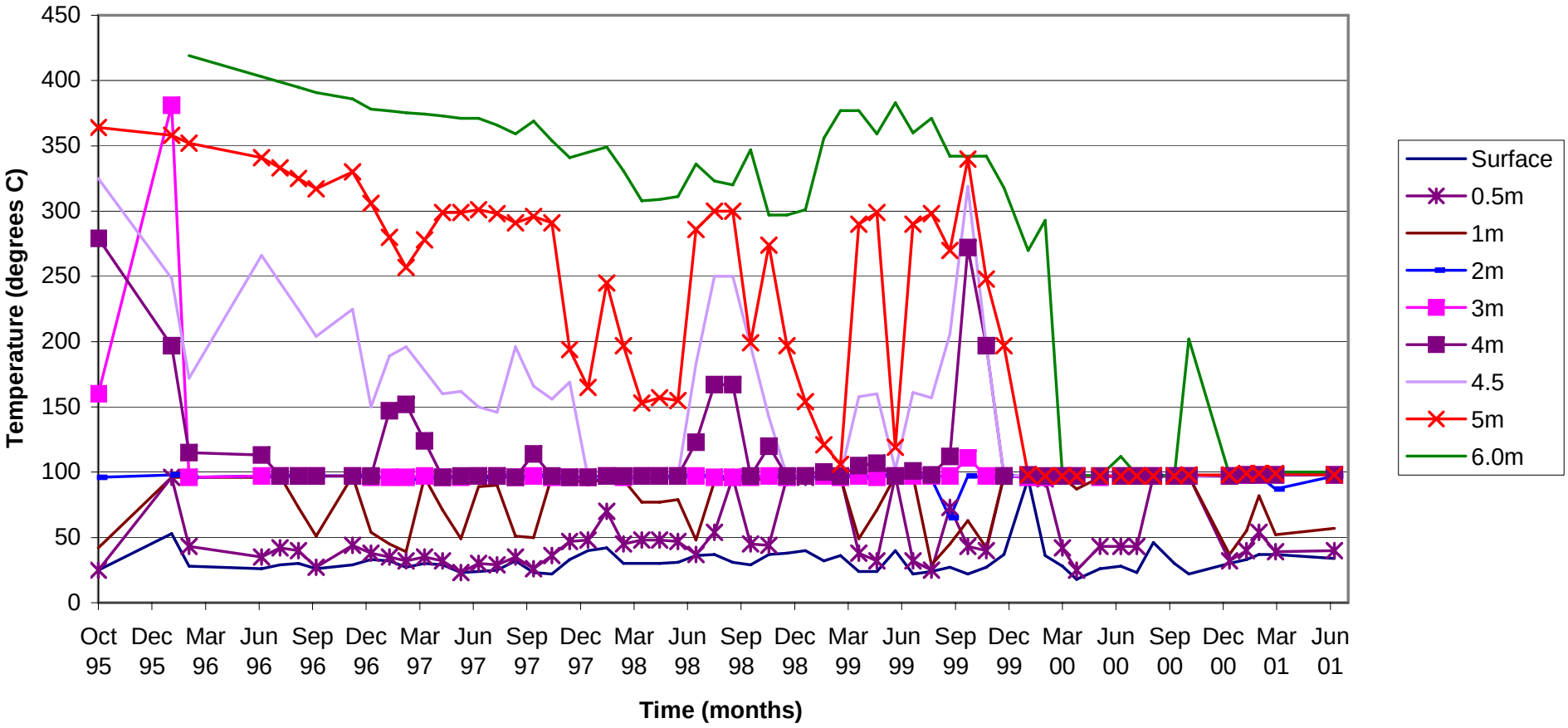

Figure 4.12 Monthly temperature variation with depth from October 1995 to June 2001 at B1/1.

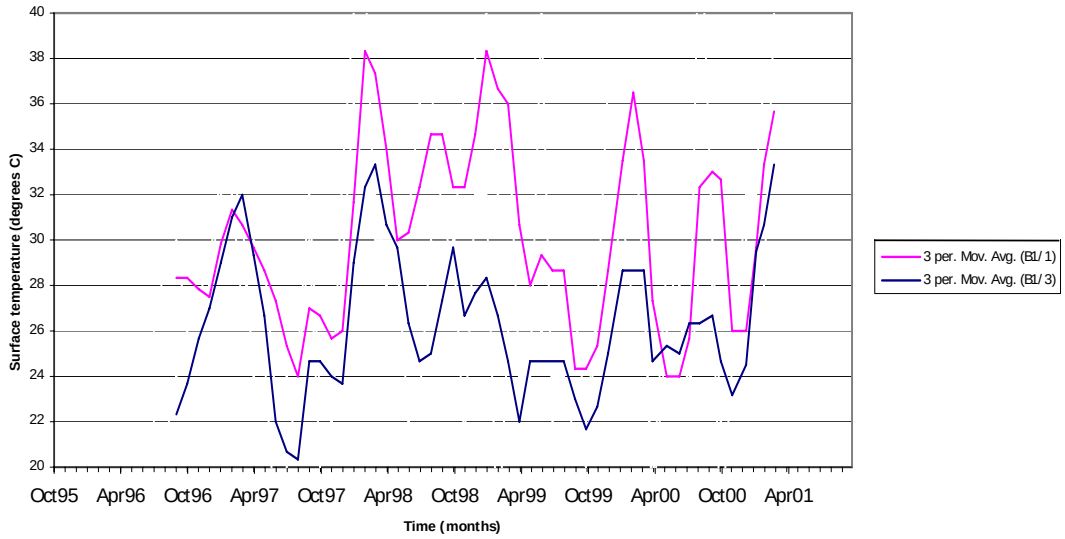

Figure 4.13 Three month moving averages of variation of surface temperature with time at B1/1 and B1/3.

The variation of temperature within the dump is displayed for October 1995 and January 1999 in **Figures 4.14** and **4.15** respectively. The figures show the relative temperatures in the dump, in sections of 1 m depths. Temperature contour plots were interpolated in Surfer using the Kriging method. The plots, especially **Figure 4.15,** displays a distinct funnelling of temperature towards a narrow exit point on the surface. This demonstrates the 'chimney effect' of gases exiting through the path of least resistance.

The monitoring data for October 1995 shows highest surface temperature at B3/2 (34°C). The fire occupies a successively larger area as one moves deeper within the dump. At 5 m below the surface, the hot spot spans over the area from B3/2 to B1/1 and B1/2.

The temperature beneath B1/1 was 364°C at a depth of 5 m below the surface. This manifested as a temperature of 25°C on the surface above that spot. At B1/2, the temperature was 24°C at the surface, and stabilises at about 95°C up to 4 m, similar to the behaviour of B1/1 at this depth seen in **Figure 4.12**. The 4 m stable temperature ranges may be due to the deposition of a different material at this level. The temperature then suddenly increases to 250°C at 5 m.

The variation in surface manifestation of the hotspot may be due to ground readings being taken during the day and the surface temperatures may reflect differential

heating on the surface. The slope and wind effects can also significantly affect surface temperatures.

The temperature contours for January 1999 are shown in **Figure 4.16**. The figure shows just the northern side of the dump where the monitoring points are sited. The surface temperature at B1/1 is 40ºC, which is significantly higher than its surrounds, which averages at approximately 29ºC. Elevated temperatures are also apparent at the surface at B3/3 (36ºC), but there are no anomalously high temperatures below the surface horizontally at B3/3 or vertically at B1/3. At 5m below the surface, the hot spot covers the area between B3/2 (143ºC), B1/2 (157ºC) and B1/1 (248ºC), but the temperatures are markedly lower than in 1995.

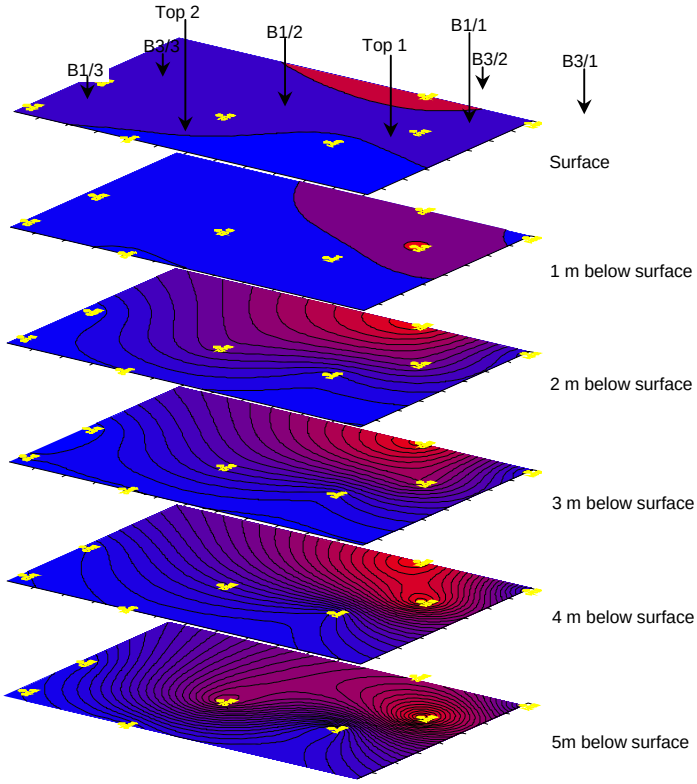

Figure 4.14 Relative variation of temperatures with depth in Dump 2 in October 1995.

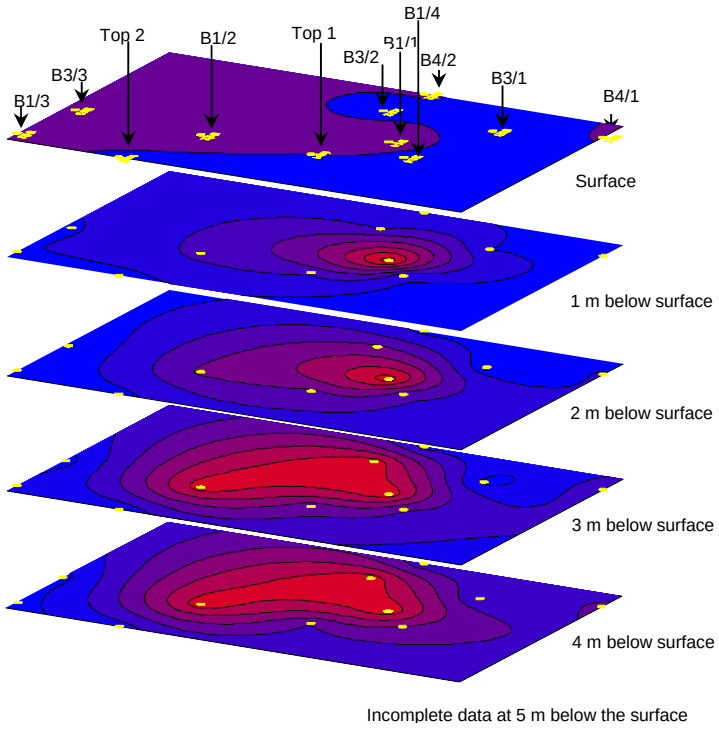

Figure 4.15 Relative variation of temperatures with depth in Dump 2 in January 1999.

Aircraft data

The nighttime flight generated the image shown in **Figure 4.16**. The hotspot on the first bench of the dump at point B1/1 is clearly evident, with some spread towards B1/2. The colours in the legend represent temperature differentials of 0.9ºC. Relative temperatures are usually given on airborne thermal imagery. Actual temperatures can be attained by calibrating the image with ground control points established at the time of flying. This image was not calibrated.

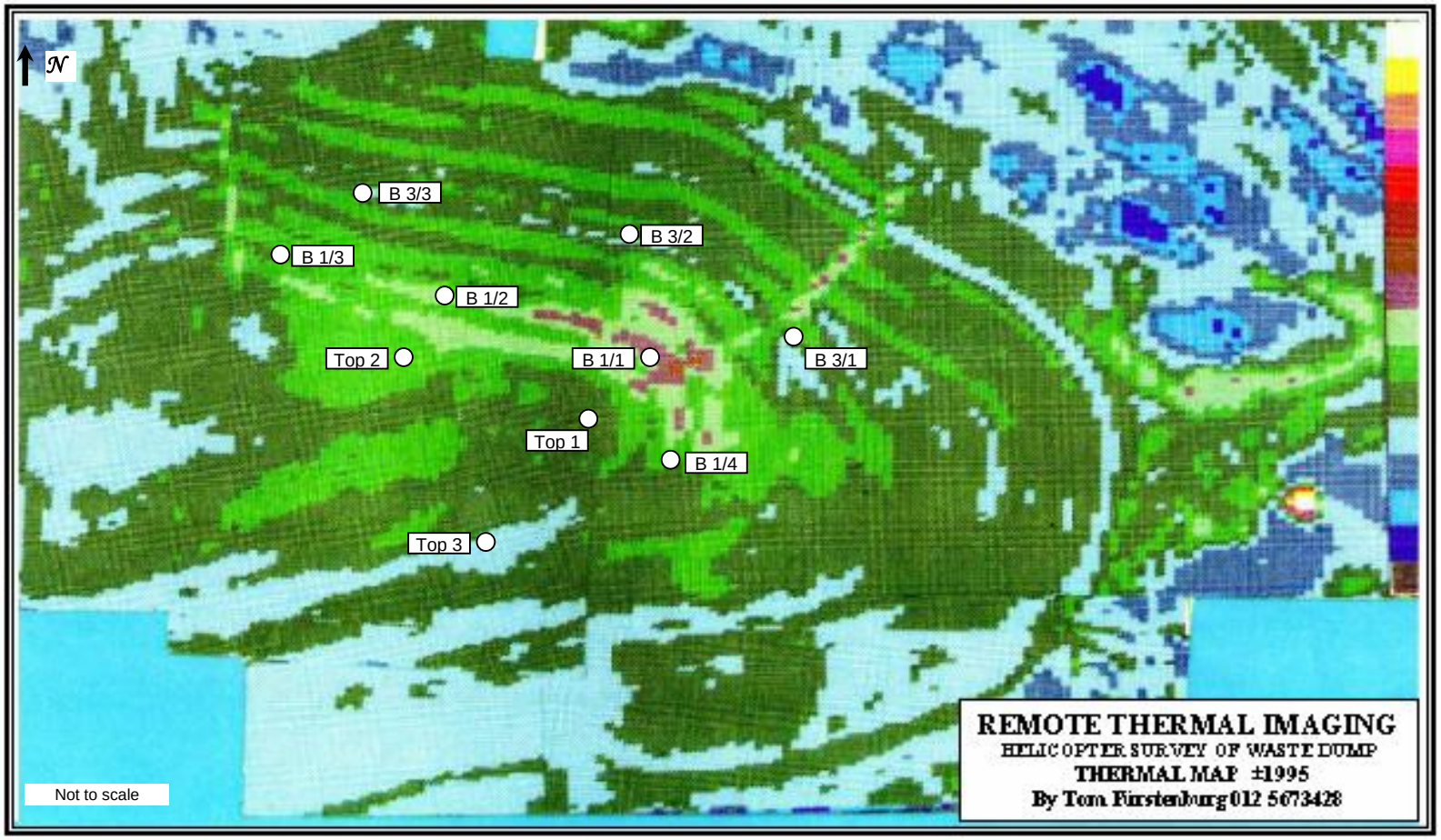

Figure 4.16 Aerial thermal survey of VCC Dump No.2 in October 1995.

Satellite data

The discard dumps were found to be extremely difficult to identify using the Landsat images. With the final dump area at 13 ha, this translates to 130 000 m^2. This can be translated to a square of 360 m. At the resolution of 120 m afforded by the thermal band, this translates to a maximum of 9 pixels (3 pixels X 3 pixels) if the dump was a perfect square and aligned to the positions of the pixels.

A colour composite of the mining area and the corresponding thermal image is shown in **Figure 4.17** and **Figure 4.18** for 1989 and 1999 respectively. The 1999 thermal image is poor and could not be used.

The change in the mining area is evident over this 10-year period. By 1999 mining had ceased and rehabilitation had progressed significantly. The thermal image for 1989 shows a number of hot spots. These are furnace houses and workshops, whose roofs heat us quickly and radiate strongly in the thermal band.

The images were taken in the morning, where the solar heating effects on the topography are significant. This effect can be taken into account by creating a digital elevation model of the site and using the sun azimuth angle to quantify the solar heating component of the image. However, this falls outside the scope of the project.

The TM6 pixel values were analysed and there were found to be no saturated pixels in the images. This implies that the maximum pixel temperature for the thermal band of 68°C was not exceeded.

It must also be borne in mind that the fires on the discard dumps were not surface fires, but sub-surface fires that manifest as only a slight warming against the ambient temperature. The image was taken at daytime, when solar heating effects are significant. At this time, the solar heating effects may mask thermal anomalies manifested by a small increase in temperature compared to the surroundings. Building a digital elevation model and modelling the solar heating effects can overcome this, but this falls outside the scope of this study.

The determination of the temperature and spread of underground fires has been documented by Zhang (1998), and Van Genderen and Haiyan (1997). For the application of monitoring discard dumps, these models are excessively resource intensive.

Zhang and Kroonenberg (1997) found that Landsat-5 TM thermal data to have too coarse a resolution for ‘early detection of coal fires with a relatively small size and low temperature’.

Figure 4.17 Landsat 5 false colour composite and thermal infrared image of VCC for 1989.

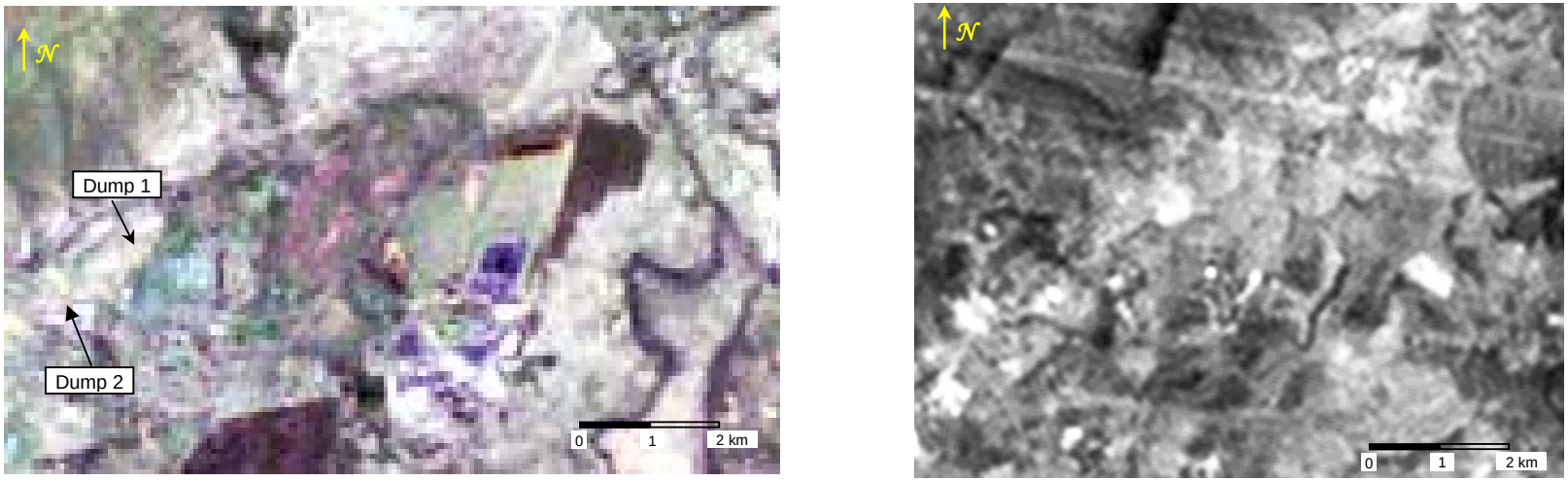

Figure 4.18 Landsat 5 false colour composite and thermal infrared image of VCC for 1999.

4.3.2 Durban Navigation Colliery (Durnacol)

Aircraft

The images from the thermal aerial survey were compiled as a video clip of the flight over the dumps. Photographs of dumps 3, 7 and 8 and stills taken from the video footage are shown in **Figures 4.19, 4.20 and 4.21** respectively**.** The hotspots on Dump 3 fringe along the bottom of the dump. The material here is loose and allows easy ingress of oxygen. The hotspots on Dump 7 are along the slopes of the dump, where the material is least compacted. The top of the dump also shows elevated temperatures. This implies the 'chimney effect', where air enters from the bottom of the dump, is heated and flows out of the top of the dump. Dump 8 has no fires. A hot spot on the west of the dump may be a pool of water that shows up warmer than the surrounding.

Photograph - Not to scale

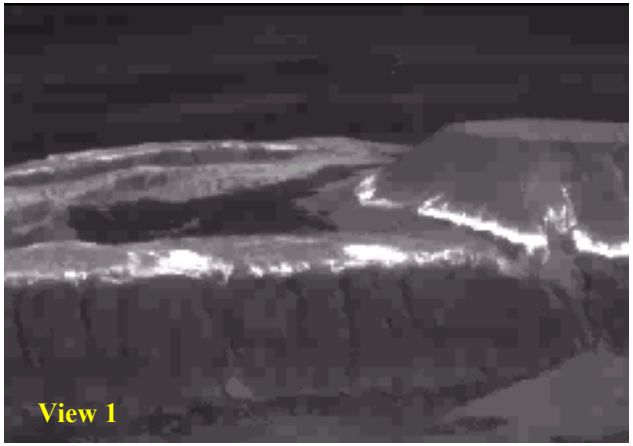

Photograph - Not to scale

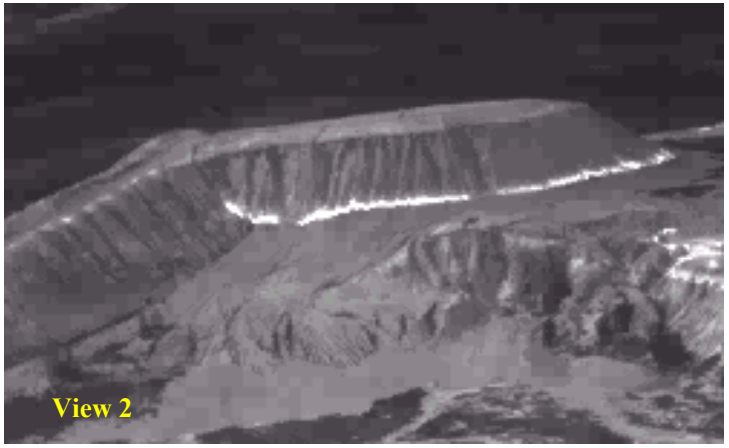

Photograph - Not to scale

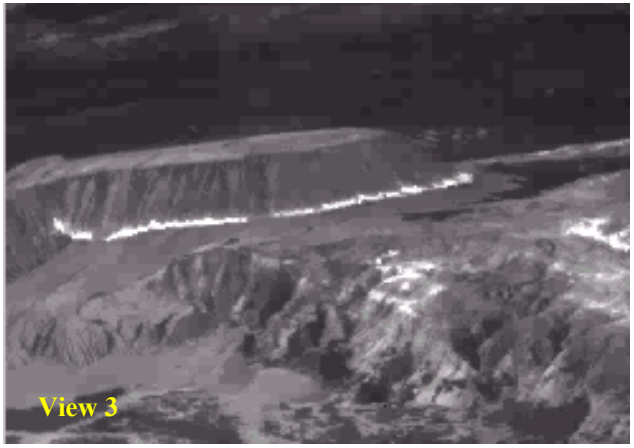

Photograph - Not to scale

Figure 4.19 Night-time airborne thermography images of Dump 3 at DNC, showing three views of the dump.

Photograph - Not to scale

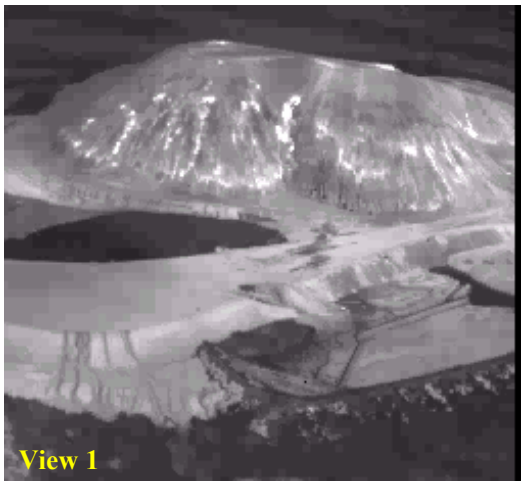

Photograph - Not to scale

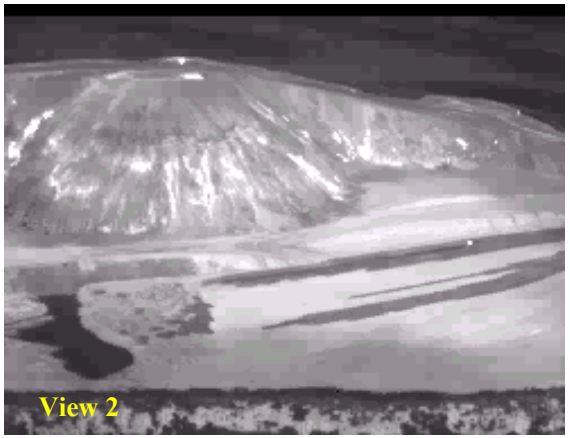

Photograph - Not to scale

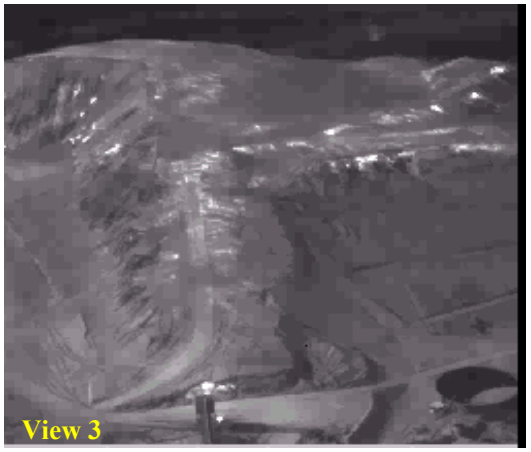

Photograph - Not to scale

Figure 4.20 Night-time airborne thermography images of Dump 7 at DNC, showing three views of the dump.

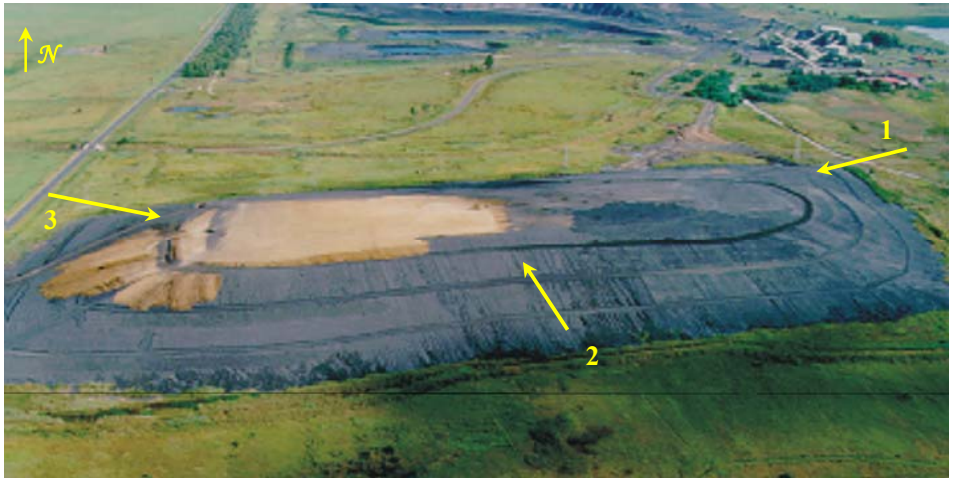

Photograph - Not to scale

Photograph - Not to scale

Photograph - Not to scale

Photograph - Not to scale

Figure 4.21 Night-time airborne thermography images of Dump 8 at DNC, showing three views of the dump.

High altitude aircraft

The MAS images were geo-referenced and a number of RGB combinations were attempted to bring out the hot spots. The composite RGB 19-10-3 was based on the principle that hot fires will radiate brightly in the short wave regions. Hot areas will therefore show red, and successively cooler areas tending towards green and blue as seen in **Figure 4.22**. The dumps appear pink, which does indicate elevated temperatures. However, the dumps are black and good absorbers of heat. Dump 8, which is being rehabilitated is known to have no fires, also appears pink in the image.

MAS has nine long wavelength thermal bands (Bands 42 to 50) in the range 8.34 μm to 14.43 μm. These bands were combined using a principle component analysis (PCA). These bands are highly correlated, and the PCA produces images that bring out the subtle difference between the bands. The first principle component is the image with the highest degree of variance and is shown in **Figure 4.23.** Although water bodies are clearly separated and appear black, the dumps are not discernable.

Harris (2001) found that MAS was suitable for detection of anomalies greater than approximately 100 m x 100 m.

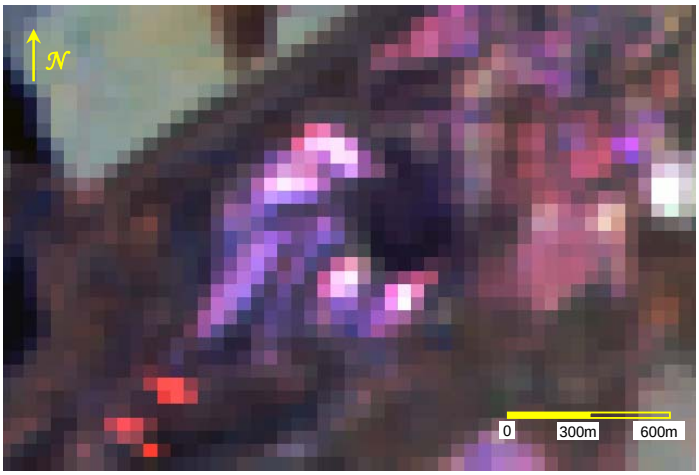

Dump 3

Dump 7

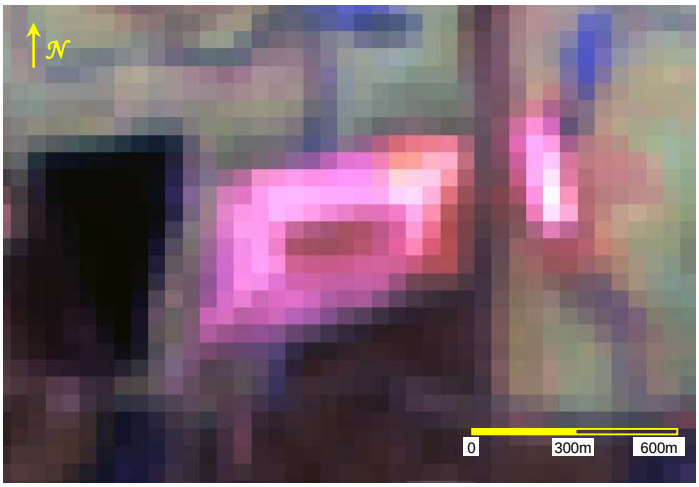

Dump 8

Figure 4.22 MAS 19-10-3 RGB composite of Durnacol discard dumps.

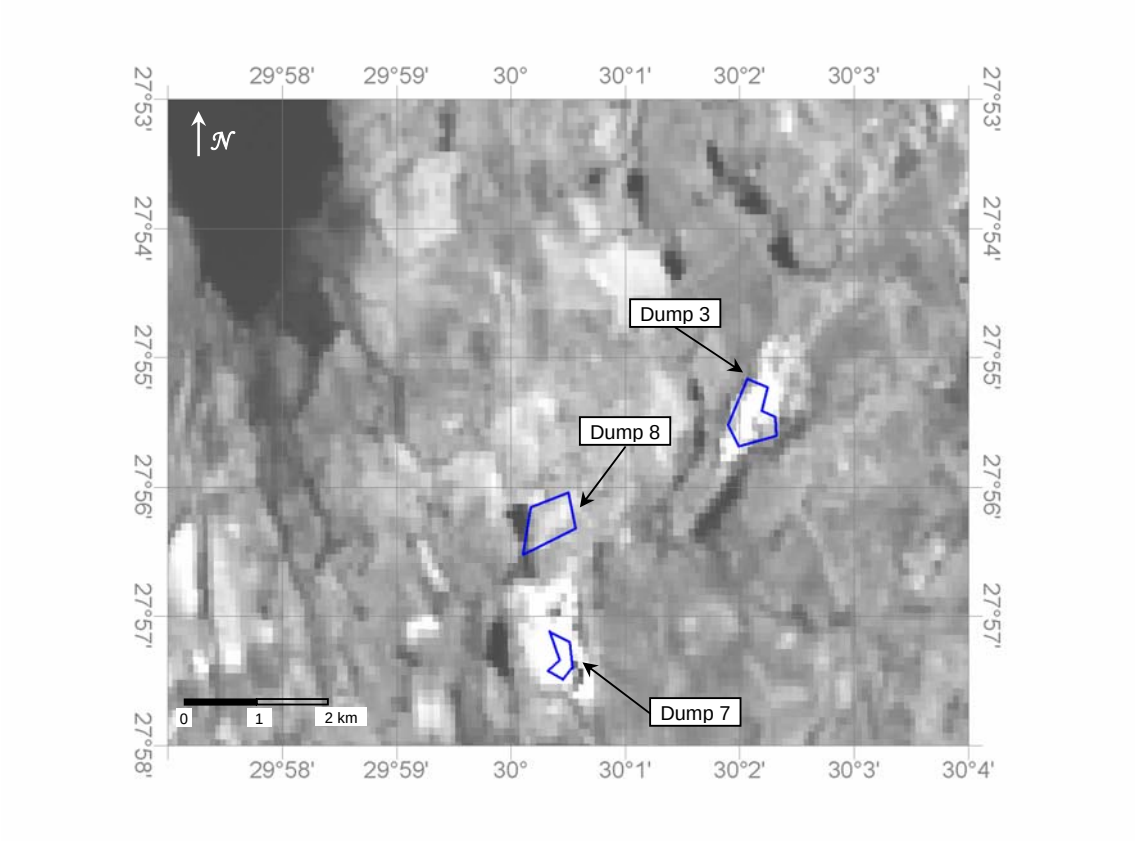

Figure 4.23 MAS first principle component image.

Satellite

The level 1 B Aster image was georeferenced. Atmospheric corrections were not applied since the longer wavelength thermal wavelengths are not affected by atmospheric effects.

Band 14, which is the longest wavelength in the thermal range collected by Aster, was contrast enhanced using a normal distribution. It was colour coded to show hot areas in red and cooler areas progressively bluer hues (**Figure 4.24**). Water is cooler than the surrounding land and appears blue. The dumps have a strong thermal signature, but it is difficult to discern variations of temperature across the surface of the dump.

SWIR and TIR images were resampled to the 15 m resolution of the VNIR using the Nearest Neighbour resampling model. RGB colour composites were created to identify fire areas. The RGB image using Bands 8, 4 and 6 are shown in **Figure 4.25**. This band combination attempts to bring out high temperature areas which reflect strongly in the short wave infrared region. Areas which appear pink are a combination of strong reflectance in Bands 8 and 6, which indicate higher

temperature anomalies. Band 4 is closer to the near infrared region, where vegetation has a strong signal. Vegetation therefore appears green.

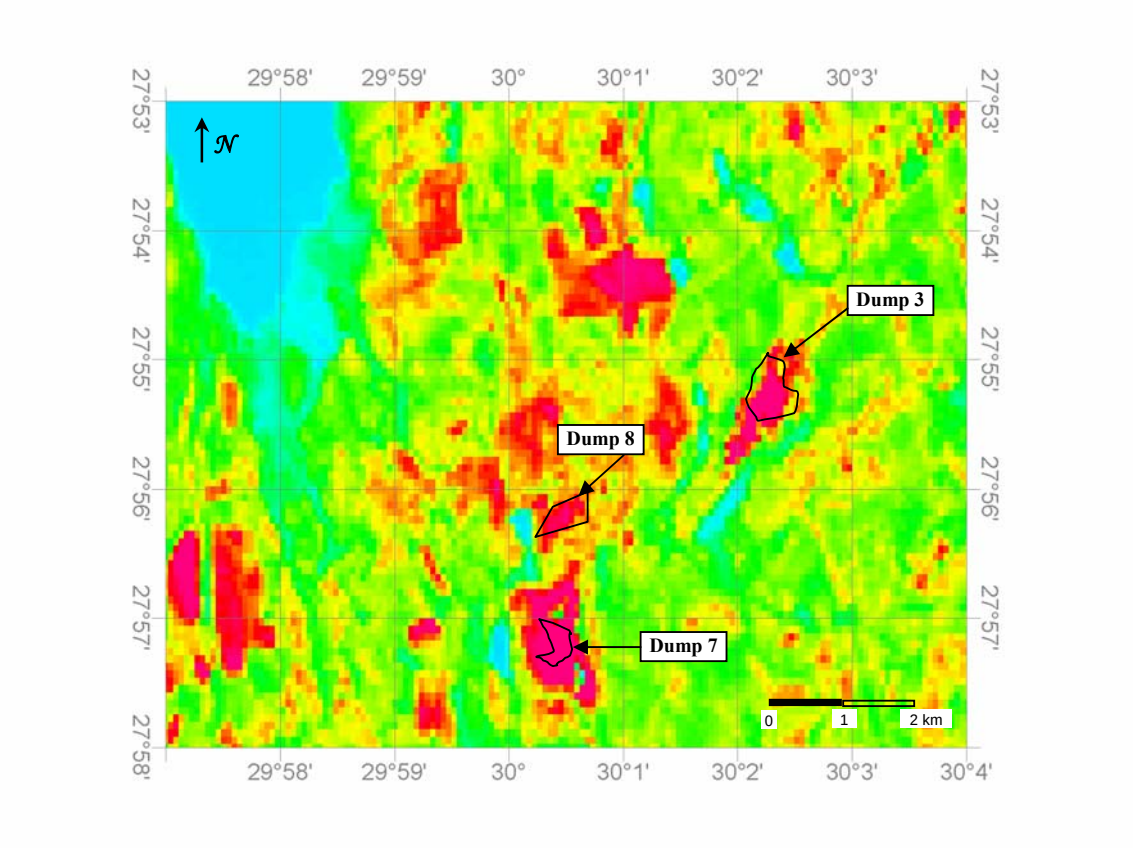

Figure 4.24 Aster Band 14 pseudo colour map.

Actual ground temperatures can be derived from satellite images if the emissivities of the ground objects can be defined. Map_SO_2 is a program developed by the NASA Jet Propulsion Laboratory to model thermal infrared signal alteration through a SO_2 plume (Rautenbach *et al*, 2003). The program produces a ground temperature map as one of its outputs.

Aster Bands 13, 12 and 11 were decorrelated and an index image created. This was used to identify emissivity classes by picking the dominant colours, which represent different ground objects or land uses. An infrared radiance image was created by combining Aster Band 10 to Band 14. A generalised DEM and model of the vertical profile of the atmosphere were obtained. These were all input into the model.

An emissivity spectrum is calculated by first defining a small 'training' region outside the plume which has a particular emissivity as identified by the decorrelated image. The emissivity spectrum is then applied to the whole image to get the ground temperature. A misfit is calculated for each pixel based on the difference between

the actual radiance measured by the sensor, and the theoretical radiance calculated from the emissivity region defined.

The model was run separately for each emissivity identified. The temperature map generated is shown in **Figure 4.26**. The map did not clearly distinguish the dumps from the surroundings, and does not show distinct temperature variation within the dump.

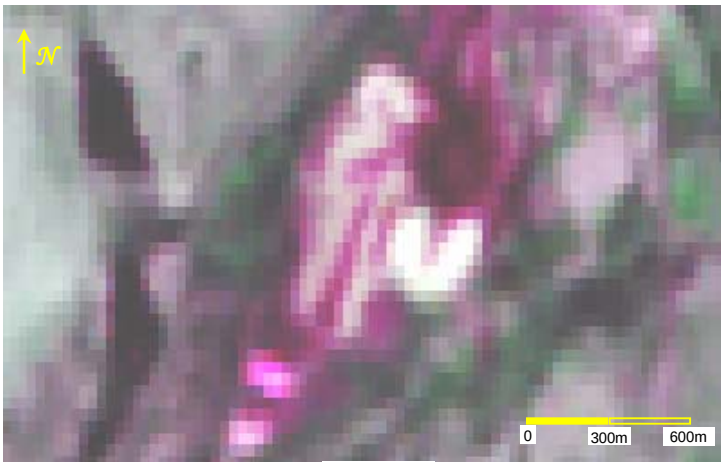

Dump 3

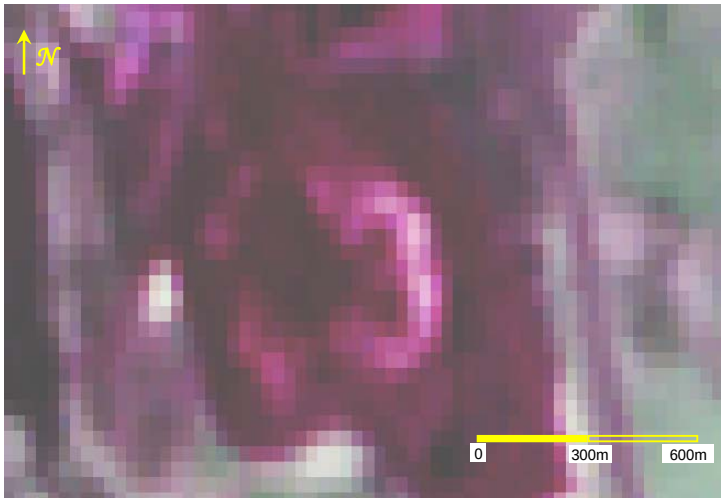

Dump 7

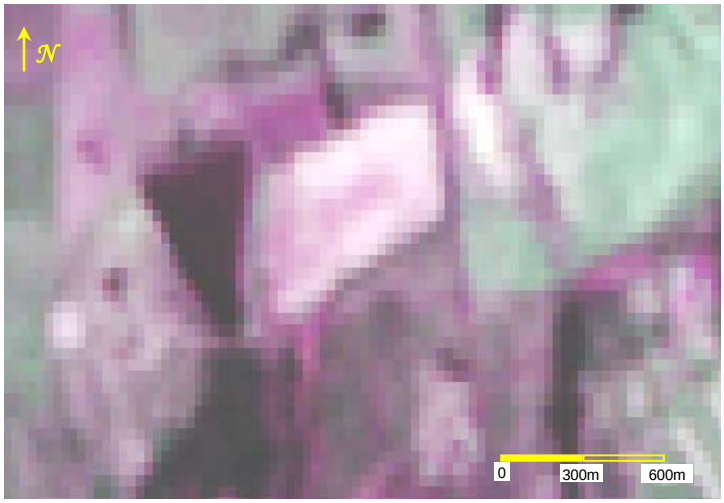

Dump 8

Figure 4.25 Aster RGB 846 combination showing close ups of each of Dump 3, Dump 7 and Dump 8.

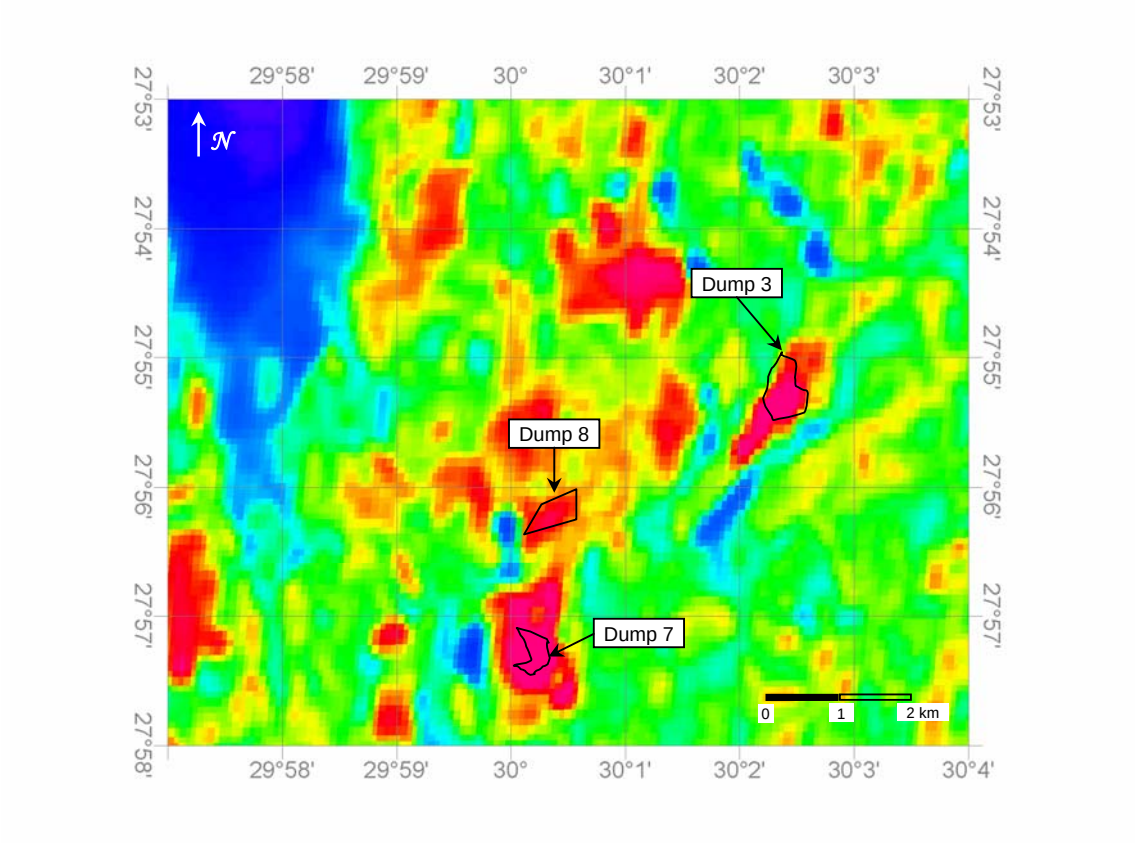

Figure 4.26 Map_SO_2 ground temperature image.

4.3.3 Kleinkopje Colliery, Witbank

The monitoring aircraft made three passes over the dump, as seen in **Figure 4.10**. For each pass, points were selected upstream of the plume, and within the plume.

The average concentrations inside and outside the plume were plotted as shown in **Figure 4.27**. The percentage change in concentration from outside to inside the plume is shown in **Figure 4.28**.The plot shows a significant increase in the concentrations of particulates, SO_2, NO and NO_2 inside the plume. These are the major pollutants commonly emitted from coal fires. The particulates are represented by numbers ranging from LPN1 to LPN 10. These are spread evenly from 0.1 to 3 µm

The large change in SO_2 (512% increase) is a sure sign of spontaneous combustion. Approximately 95 % of the sulphur in bituminous coal is converted to SO_2 during combustion (US EPA, 1998). The sulphur oxides originate from the oxidation of the organic and pyritic sulphur in the coal during combustion (US EPA, 1998).

A reduction in O_3 is evident inside the plume. Percentage change in small particulates is greater than larger particulates, up to LPN8. This indicates that the underground fire may cause filtering of larger particles as the smoke moves up through the overlying material.

Figure 4.9 indicate that there is no significant change in CO and CO_2 levels in the plume. The detection of these may be limited by the sensitivity of the sensor. A closer inspection of the CO_2 levels in the plume (**Figure 4.10**) show a sharp increase in concentration from one point to another, followed by a sharp drop off at the next point. The readings are taken one second apart, and the aircraft speed is approximately 100 m/s. Therefore the plume of 400 m is represented by only 4 points. The sensor may have missed the CO2 peak.

The levels of NO and NO_2 within the plume are 69% and 41% higher than the background levels. Elevated NO_x can originate from the oxidation of organic N bound in the coal.

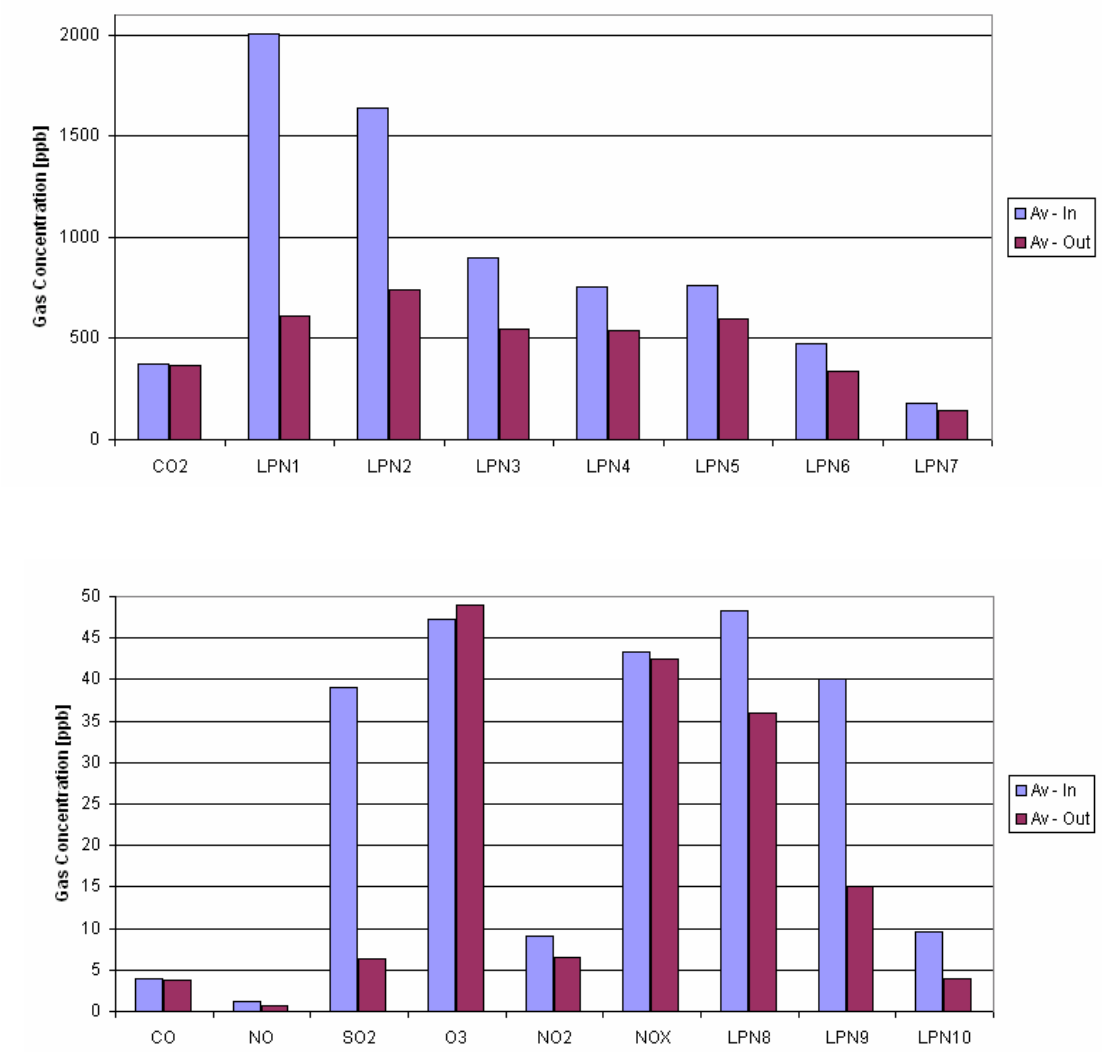

Figure 4.27 A comparison of average concentrations of gases and small particulates inside and outside the smoke plume.

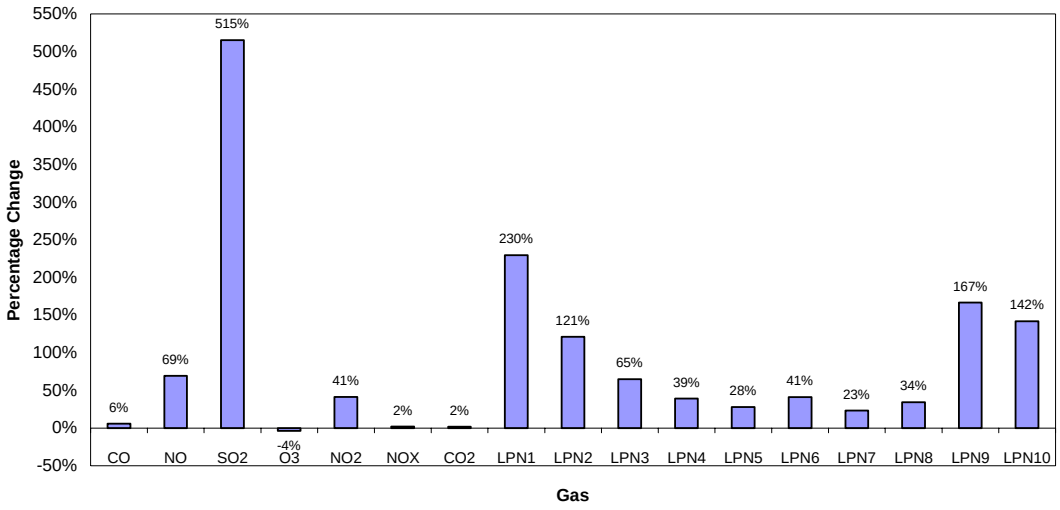

Figure 4.28 Percentage concentration change from upstream to inside of the plume.

CHAPTER 5 CONCLUSIONS

5.1 Conclusion

Four levels of thermal monitoring data were assessed in this project. These were: ground and below surface temperature probes; aerial thermal and atmospheric monitoring surveys; high altitude aircraft; and satellites. These are compared in **Table 5.1** in terms of detection ability and data availability, the level of available data and the cost.

Although aerial thermal surveys are expensive to conduct, they present the best resolution of data for the detection of the position and relative temperature of the fire on individual discard dumps. Specific areas can be flown and the exact position of any thermal anomalies can be determined.

It must be noted that remote sensing methods measure only variation of temperatures on the surface. Fires on discard dumps are sub-surface fires, and the depth and extent of the fire below the surface cannot be easily inferred. This makes the planning of rehabilitation efforts difficult and dangerous. Therefore, remote sensing tools should not be exclusively used to assess fires on discard dumps. Ground monitoring must be conducted before rehabilitation works are planned.

Satellite data are readily available, and the information contained in the image can be used for various other monitoring purposes on a mine. These include monitoring vegetation on rehabilitated areas, monitoring seepage flows and acid mine drainage and monitoring the progress of mining and adjacent land use changes.

The resolution of the sensors is a limiting factor for detecting individual hotspots on dumps (ground resolution of 120 m for Landsat 5 and 90 m for ASTER thermal channels). Small mine dumps occupy just a few pixels and the position of fires cannot be accurately assessed. Although the larger dumps are discernable, the variation of temperatures across the dump cannot be easily determined. Even at the resolution of 50 m afforded by the high altitude MAS sensor, the individual hotspots were not easily discernable.

Solar heating effects must be taken into account for daytime images. Sun facing slopes appear bright in thermal images, even though there may be no fires in the area. Uncovered dumps are black and tend to absorb heat quickly during the day, making it difficult to identify thermal anomalies. Daytime emissions through the surface from sub surface fires are unlikely to exceed the natural solar heating effects on the dumps. A surface temperature of only 4˚C higher than ambient was observed

on a dump where subsurface probes showed a substantial underground fire with temperatures up to 424˚C at 6 m depth.

Although satellite remote sensing may be a valuable tool for mine monitoring in the future, as ground resolutions improve, its application at present is hampered by the coarse resolution of the sensors relative to the small size of the fires. **Figures 4.14 and 4.15** illustrate that even substantial underground temperature anomalies, down to depths of 6 m below the surface, manifest as much smaller hotspots at the surface. This is possibly due to the hot gasses moving along paths of least resistance, promoting the formation of a chimney.

Aerial atmospheric monitoring surveys are also able to detect the presence of fires on discard dumps. However, this method is a less direct method and not suited to routine monitoring on mines.

Table 5.1 Comparison of the thermal data sets used in this project.

	Ground monitoring	Thermal aerial survey	High altitude aircraft	Landsat	ASTER
Detection ability and data availability	• Minimum monthly monitoring required. • Staff must be trained and to take readings accurately. Human error in reading likely. • Method is time intensive - Time needed for thermocouples to equilibrate • Data must be kept and analysed on a regular basis. • Not suitable for once off monitoring	• Suitable for once off monitoring or on a as needed basis • Specialist required to conduct the survey • Good ground resolution • Night time flights eliminate solar heating effects and make anomalies easy to see	• Data is not commercially available	• Suitable for once off monitoring or on a as needed basis. • Image acquisition restricted to the satellite overpass time and available at a maximum of one image every 16 days. • An image cannot be used for days of excessive cloud cover • Specialist expertise and software required to analyse images • Ground resolution poor for detection of sub-surface fires on small dumps. • Morning overpass, after sunrise, of the satellite, results in solar heating effects	• Suitable for once off monitoring or on an as-needed basis. • Image acquisition restricted to the satellite overpass time • Aster collects a limited number of images daily. Images are not acquired continuously and requests can only be made by registered ASTER users. • Requests must be made at least 6 months in advance. • An image cannot be used for days of excessive cloud cover • Specialist expertise and software required to analyse images • Ground resolution poor for detection of sub-surface fires on small dumps. • Morning overpass, after sunrise, of the satellite, results in solar heating effects

	Ground monitoring	Thermal aerial survey	High altitude aircraft	Landsat	ASTER
Level of available data	• Detailed data available on fire depth and actual temperatures are obtained. • This level of detail may not be necessary for monitoring purposes • Any spatial resolution is possible, horizontally and vertically.	• Relative temperatures are obtained. Determination of actual temperatures possible, at additional cost. • Actual positions of the fires on the dumps can be accurately determined. • Ground resolution between 0.5 – 1 m	• The instrument collects data on a large number of narrow spectral bands. This level of spectral resolution is not necessary for the application studied. • Ground resolution 50 m	• Visible, infrared and thermal bands can provide a great deal of information about the mine site, including vegetation growth on rehabilitated areas, areas of degradation, acid mine drainage, seepage effects etc. • Relative temperatures can easily be determined from thermal bands using simple processing techniques. • Actual temperatures can be attained by applying algorithms to convert radiance to temperature. • Easily available from USGS DAAC or locally at the CSIR • Ground resolution 120 m (thermal)	• Visible, infrared and thermal bands can provide a great deal of information about the mine site, including vegetation growth on rehabilitated areas, areas of degradation, acid mine drainage, seepage effects etc. • Relative temperatures can easily be determined from thermal bands using simple processing techniques. • Higher-level products can be attained on request, including ground temperatures. • Ground resolution 90 m (thermal)
Cost	R12 000- R15 000 set-up cost plus additional operation and maintenance costs	R30 000 per flight	Not available for commercial use	R5 000 per scene (up to 625 km^2)	R550 per granule

5.2 Further research

A key to understanding and applying remote sensing techniques to the monitoring of coal discard dumps is the ability to model the thermal behaviour of the dumps. Surface thermal anomalies must be translated to the depth and extent of the actual fire below the surface. A study of the physical characteristics of the dump, such as material type, shape, depth of placement and degree of compaction, together with the outside environmental conditions, for example temperature and pressure, will provide valuable information on the thermal mechanics of the system.

REFERENCES

Anderson J E and Robbins E I (1998) *Spectral Reflectance and Detection of Iron-oxide Precipitates Associated with Acidic Mine Drainage*. Photogrammetric Engineering and Remote Sensing, Vol. 64, No12, pp1201-1208.

Bassier R, Clostermann M, Kappernagel T (2000) *Environmental Challenges in Mine Closures in Germany*, Coal-The Future, 12th International Conference on Coal Research, South African Institute of Mining and Metallurgy, Sandton, Johannesburg, September 2000.

Bell F G (1996) *Dereliction: Colliery Spoil Heaps and their Restoration*, Environmental and Engineering Geoscience, Vol 2, No1, pp 85-96.

Bell F G, Bullock S E T, Hälbich T F J, Lindsay P (2001) *Environmental Impacts Associated with an Abandoned Mine in the Wibank Coalfield, South Africa*. International Journal of Coal Geology, Vol 45, pp 195-216.

Bennetts R (1992) *Mastering the Monoliths*, SA Mining, Coal & Gold Base Minerals, June 1992, pp 15-17.

Bezuidenhout N, Van Niekerk A M and Vermaak J J G (2000) *The Effects of Natural Soil Covers on Geochemical Processes Associated with Coal Discard Deposits - Results from a Pilot Scale Study*. Proceedings from the 5thInternational Conference on Acid Rock Drainage, Colorado, USA.

Böhm C, Kühnen A and Niederhuber M (2000) *Application of Earth Observation Data in Monitoring and Recultivation of Mining Areas*. Proceedings of 28th International Symposium on Remote Sensing of Environment, 27-31 March 2000, Cape Town, South Africa.

Chamber of Mines (2001) http://www.bullion.org.za/welkome.htm Accessed 8/09/2000

Chevrel S and Coetzee H (2000) *A New Tool for Assessing the Environmental Impact of Mining Activities - Application to the Surface and Groundwater Sensitivity Analysis of the West Rand area – Gauteng Province – South Africa*. Proceedings of 28th International Symposium on Remote Sensing of Environment, 27-31 March 2000, Cape Town, South Africa.

Colliery Guardian (1994) *Rehabilitation of a South African Coal Dump*. May 1994, pp104-107.

Eroglu N (1999) *Developing methods to prevent and control spontaneous combustion associated with mining and subsidence*. Coaltech 2020 Interim Report, Miningtek, CSIR, Johannesburg.

Farquharson D C, Richter J and Furstenburg T A P (1992) *Spontaneous Combustion of Discard from an Open Cast Coal Mine: A Large Scale Test*. ISKOR; Unpublished.

Garner R D, Tanner P and Aken M (2001) *Rehabilitation of Discards: A Case Study of the Springbok Valley*, Proceedings of the Conference on Environmentally Responsible Mining in Southern Africa, 25-28 September 2001, Muldersdrift, Johannesburg.

Gillespie A, Rokugawa S, Matsunaga T, Cothern J S, Hook S, Kahle A B (1998), *A Temperature and Emissivity Separation Algorithm for Advanced Spaceborne Thermal Emission and Reflection Radiometer (ASTER) Images*. IEEE Transactions on Geosciences and Remote Sensing, Vol 36, No 4, pp 1113-1126.

Grobbelaar C J, Surridge A D, Asamoah J K (1995) *Strategy for the Management and Utilization of Discard Coal and Fines*. Proceedings of the South African Institute of Mining and Metallurgy Colloquium: Coal Processing, Utilisation and Control of Emissions, Johannesburg, March 1995.

Harris R (1987) *Satellite Remote Sensing: An Introduction*, Routledge & Kegan Paul, London.

Harris R W (2001) Personal communication, Geodatec Pty Ltd, (011) 765 – 3254.

Hocking A (1995) *Durnacol – The Story of Durban Navigation Collieries*. Hollards Corporate, South Africa.

Holding W (1994) *Review of Practices for the Prevention, Detection and Control of Underground Fires in Coal Mines*. Safety in Mines Research Advisory Committee (SIMRAC), Final Project Report No COL 031.

Kural O (1994) *Coal: Resources, Properties, Utilization, Pollution*. Mining Faculty, Istanbul Technical University, Turkey.

Landman T (2003) *Characterising Sub-Pixel Landsat ETM+ Fire Severity on Experimental Fires in the Kruger National Park, South Africa.* South African Journal of Science, No 99, July/August 2003.

Lillisand T M and Keifer R W (2000) *Remote Sensing and Image Interpretation*, 4th Edition, John Wiley and Sons, New York.

Limpitlaw D, Aken M and Van Zyl H C (2000) *Monitoring Coal Mine Rehabilitation Using Satellite Data*, Proceedings of Coal – The Future, 12th International Conference on Coal Research, South African Institute of Mining and Metallurgy, Sandton, Johannesburg, September 2000.

Liu C L, Li S S, Qiao Q D, Wang J S, Pan Z Q (1998) *Management of Spontaneous Combustion in Coal Mine Waste Tips in China*. Water Air and Soil Pollution, Vol 103, pp 441-444.

Luckos A (2002) *Formation of Emissions in Industrial Combustion and Power Generation and Metallurgical Processes*, Proceedings of Coal and the Environment, Pre-Conference to the World Summit on Sustainable Development, 5-8 August 2002, Randburg, South Africa.

Master S and Woldai T (2001) *Application of Multi-temporal ERS-1 Synthetic Aperture Radar Imagery in Mapping Mining Related Land Use, Environmental Degradation and Hydrology in the Kolwezi Cu-Co mining region, Katanga, Democratic Republic of Congo*. Proceedings on the Conference on Environmentally Responsible Mining in Southern Africa, Chamber of Mines, South Africa, Muldersdrift, Johannesburg, March 2001.

Mbendi (2005) http://www.mbendi.co.za/indy/ming/coal/as/cj/p005.htm, accessed 10/10/05

Prakash A and R.P (1999) *Surface Fires in Jharia Coalfield, India – Their Distribution and Estimation of Area and Temperature from TM Data*, International Journal of Remote Sensing, Vol 20, No 10, pp 1935-1946.

Prakash A, Gupta R P and Saraf A K (1997) *A Landsat TM Based Comparitive Study of Surface and Subsurface Fires in the Jharia coalfield, India*. International Journal of Remote Sensing, Vol 18, No 11, pp 2463-2469.

Prakash A, Saraf A K, Gupta R P, Dutta M and Sundaram R M (1995) S*urface Thermal Anomalies Associated with Underground Fires in the Jharia Coal Mines, India.* International Journal of Remote Sensing, Vol 16, No 12, pp 2105-2109.

Rautenbach C, Kneen M. A, Annegarn H. J and Realmuto V.J (2003) *Satellite Remote Sensing of Industrial Sulphur Dioxide Plumes*, MSc Research Report, University of the Witwatersrand, Unpublished.

SA Mining, Coal & Gold Base Minerals (1992) *Putting Paid to Pollutants at JCI*. June 1992, p 21.

SA Mining, Coal & Gold Base Minerals (1994) *Seeking a Solution*. June 1994, pp 17-18.

Sabins F F Jr (1987) *Remote Sensing Principles and Interpretation*, 2nd Edition, W H Freeman and Company, New York.

South African Government (2005) http://www.info.gov.za/aboutsa/minerals.htm, accessed 10/10/2005

US EPA (1998) *Compilation of Air Pollutant Emission Factors*, AP-42, 5th Edition, Vol 1.

Unal S (1995) *A Review of Spontaneous Combustion of Coals*. Fuel, Science and Technology International, Vol 13, No 9, pp 1103 – 1120.

Van Genderen, J L and Haiyan, G (1997) *Environmental Monitoring of Spontaneous Combustion in the North China Coalfields*, Final Report to European Commission, Contract No CI1*-CT93-0008 (DG-HSMV).

Vermaak J J G and Bezuidenhout N (2000) *Design of Soil Covers as Oxygen Barriers for the South African Climate*. Proceedings of the South African Young Geotechnical Engineers Conference, Stellenbosch, September 2000.

Wade L (1988) *The Propensity of South African Coals to Spontaneously Combust*. PhD Thesis, University of the Witwatersrand, unpublished.

Wates J A, Vermaak J J G and Bezuidenhout N (2000) *Design of Soil Covers to Reduce Infiltration on Rehabilitated Opencast Coal Mines*, Proceedings of the Fourth Environmental Management, Technology and Development Conference, Johannesburg, South Africa.

Zhang X (1998) *Coal Fires in Northwest China – Detection, Monitoring and Prediction Using Remote Sensing Data*. PhD Thesis, Technische Universiteit Delft, ITC Publication No 58.

Zhang X and Kroonenberg S B (1997) *A Method to Evaluate the Capability of Landsat-5 TM Band 6 data for Sub-pixel Coal Fire Detection*, International Journal of Remote Sensing, Vol 18, No 15, pp 3279-3288.

Appendix 1:
Vryheid Coronation Colliery Dump No.2 Underground Temperature Monitoring Data